이학석사학위논문

Single-molecule Fluorescence Study for the Effects of DNA Methylation on the Association and Dissociation Kinetics of Restriction Endonuclease and DNA

DNA 메틸화가 제한효소와 DNA 결합 및 분해
동역학에 주는 영향에 대한 단분자 형광 연구

2014년 2월

서울대학교 대학원

화학부 물리화학전공

박 소 영

MS. Dissertation

Single-molecule Fluorescence Study for the Effects of DNA Methylation on the Association and Dissociation Kinetics of Restriction Endonuclease and DNA

February 2014

Research Advisor:

Professor Seong Keun Kim

Department of Chemistry

Seoul National University

So Young Bak

Abstract

Single-molecule fluorescence study for the effects of DNA methylation on the association and dissociation kinetics of restriction endonuclease and DNA

So Young Bak

Department of Chemistry

The Graduate School

Seoul National University

DNA methylation plays a great role both in eukaryotic and prokaryotic cells. In eukaryotes, it suppresses gene regulation, whereas in prokaryotes, specifically in bacteria, it protects the cell from invasion of foreign genes. Many studies have been carried out for the effect of DNA methylation at the ensemble level, but in this study, we investigated the effect of DNA methylation on DNA-protein interaction by single-molecule fluorescence to understand the interaction at the molecular level. We measured the association and dissociation rates of native as well as methylated DNA and found that the values converge to the corresponding ensemble rates. We were able to differentiate the kinetics of association, and dissociation and found that our result was consistent with the fact that DNA methylation interrupts the DNA- protein interaction, especially at a specific kinetic

step.

Keywords: Single-molecule technique, Total internal reflection fluorescence microscopy, Restriction endonuclease, *Hin*dIII, Protein-DNA interaction, DNA methylation

Student Number: 2011-23221

Table of Contents

1. Introduction

Observation and detection of kinetics and dynamics of biomolecules have drawn attention to many scientists because understanding the phenomena of the biomolecules are intimately related to humans. These are mostly studied in bulk materials, in which the kinetics of the hundreds and thousands of biomolecules are averaged out in ensemble and show the trend of a majority in a condition. The desire to scope down to an individual molecule and observe the kinetics of one molecule has developed the single-molecule technique. The single-molecule technique allows us to solve our curiosity of observing the hidden steps of protein kinetics that otherwise are indistinguishable at the ensemble level.[1] While ensemble tests provide an averaged value, a single-molecule technique distinguishes one molecule at a time and gives information of kinetics and conformational changes of proteins and DNA.

Single-molecule tools are put in a category by various standards. Total internal reflection fluorescence microscopy, TIRF, is categorized as an immobilization-based technique that is one of the most popular single-molecule techniques that draws a trajectory of a single molecule while it is immobilized on a surface of a quartz. The immobilized molecules are generally labeled with a fluorescence dye, and the fluorescence dye molecules are visualized when the dye molecules are excited by evanescent wave that is generated at the interface of the quartz and the aqueous solution.

In this study, we used TIRF to observe the kinetics of restriction endonuclease, *Hin*dIII. The experiment was designed to employ the photophysical property of Cy3 rather than FRET which is another popular way of detecting kinetics of proteins. Through analysis of the observed association and dissociation, the effects of methylation can be elucidated.

2. Basic Principles

2.1 Total internal reflection fluorescence microscopy

Optical configurations

Total Internal Reflection Fluorescence, TIRF, is a type of fluorescence assay that detects the kinetics of a single molecule at a low concentration. We used a diode laser (532nm) with 100mW (TECGL-30, World Star Tech.). The light passes through the Pellin Broca Prisms (PLBC-5.0-79.5-SS) and the fluorescence of the samples are excited by evanescent field generated by total internal reflection. The fluorescence enters the EMCCD (Andor; DU-897E-CS0-#BV) with exposure time of 100 ms and visualized by IDL software. The visualized molecules are analyzed with MATLAB program. Through selective excitation of the immobilized fluorophores, TIRF enables to track a single molecule for a range of time with high signal-to-noise ratio. Figure 1 is the scheme of the setup.

Total internal reflection fluorescence

When light travels from a higher refraction index medium to a lower refraction index medium, the light changes its pathway according to Snell's law. If the incident angle is greater than the critical angle, the light does not pass through the medium, but totally reflects. Total internal reflection induces an electromagnetic field of evanescent field which decays exponentially from an interface of a quartz. The penetration depth of TIRF is shallow (~150 nm) and excites the fluorophores which are immobilized in the range of ~150 nm from the surface of the quartz. The characteristic of exponential decay of evanescence field avoids the background noise from the fluorophores which are not immobilized, and improves the signal-to-noise ratio critically.

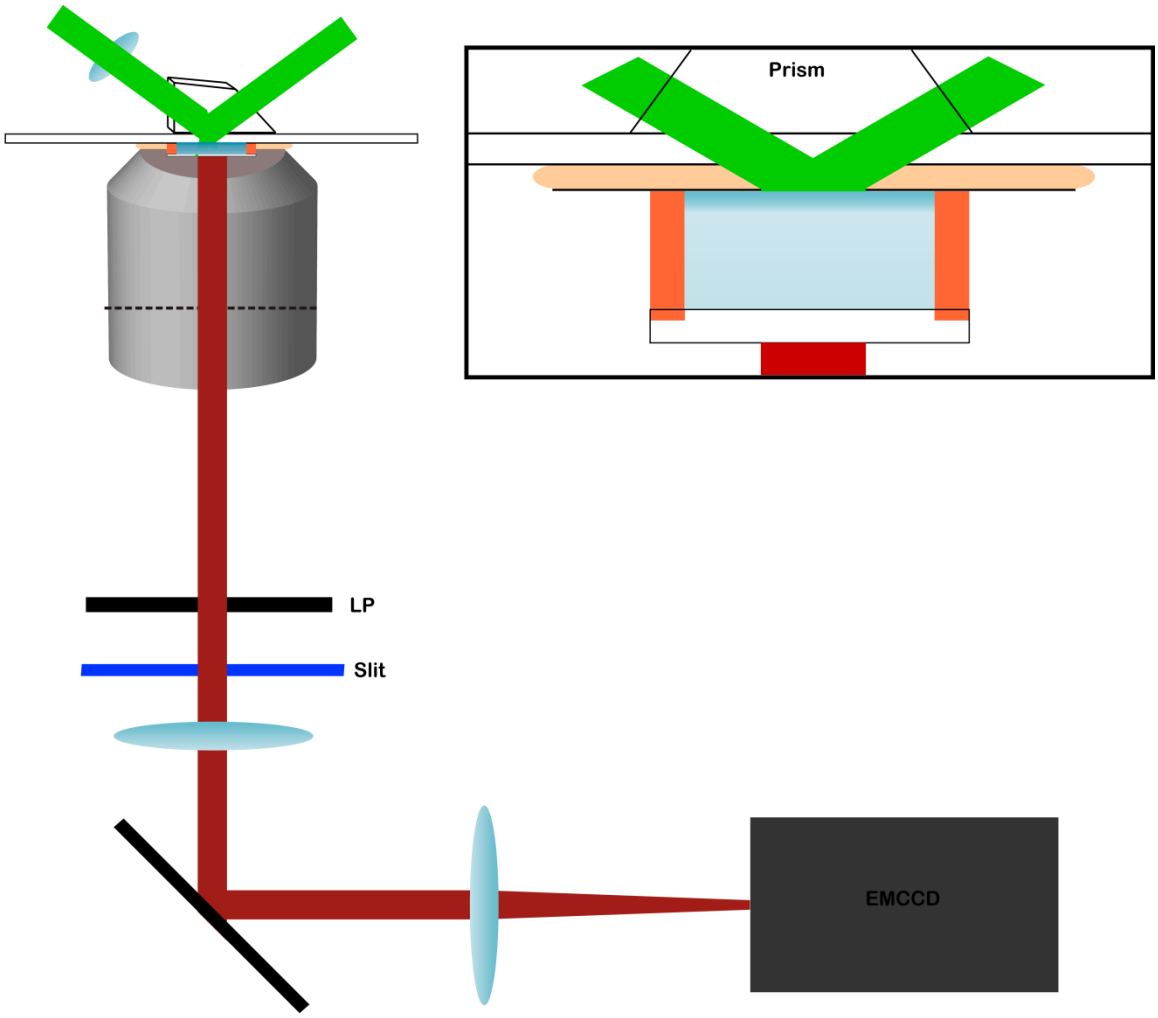

Figure 1. Scheme of the TIRF setup. Green ray indicates the laser source (532 nm), the blue area indicates the evanescent field generated from total internal reflection, and the LP stands for long pass filter.

Prism-based TIR.

Prism is used to generate the total internal reflection and evanescent field. The refractive index of prism is about 1.45 which is close to that of quartz. The immersion oil with refractive index 1.45 is used to eliminate any refractive index difference. The incident light passes through a prism, quartz and then on the surface of aqueous buffer with refractive index 1.33, it deflects according to Snell's law. Snell's law is applied as below:

$$n_1 \sin \Theta_1 = n_2 \sin \Theta_2$$

$$\sin \Theta_1 = \frac{n2}{n1} = \frac{1.33}{1.45}$$

$$\Theta_1 = 66.5^{\circ}$$

Θ_2 is 90 degrees at a critical angle. When incident angle is steeper than the critical angle, 66.5˚, the light totally reflects, and generates the evanescent field.

Evanescent field is an electromagnetic field that penetrates into the liquid medium between a quartz and coverslip. *I* is an intensity and *z* is the perpendicular distance from the surface of a quartz.

$$I = I_0 \exp(-\frac{z}{d})$$

$$\mathrm{d} = \frac{\lambda}{4\pi n_2}\left(\frac{sin^2\,\theta}{sin^2\,\theta c} - 1\right)^{-1/2}$$

d is the exponential decay depth, θ_c is the critical angle of incidence, θ is the angle of incidence light, λ is the wavelength of incident light in vacuum, and n_2 is the refractive index of the aqueous medium in our case. θ should be greater than θ_c. This equation drives that the depth of evanescent field increases with decreasing θ. The depth of the evanescent field can be controlled by the angle of incidence light.[2]

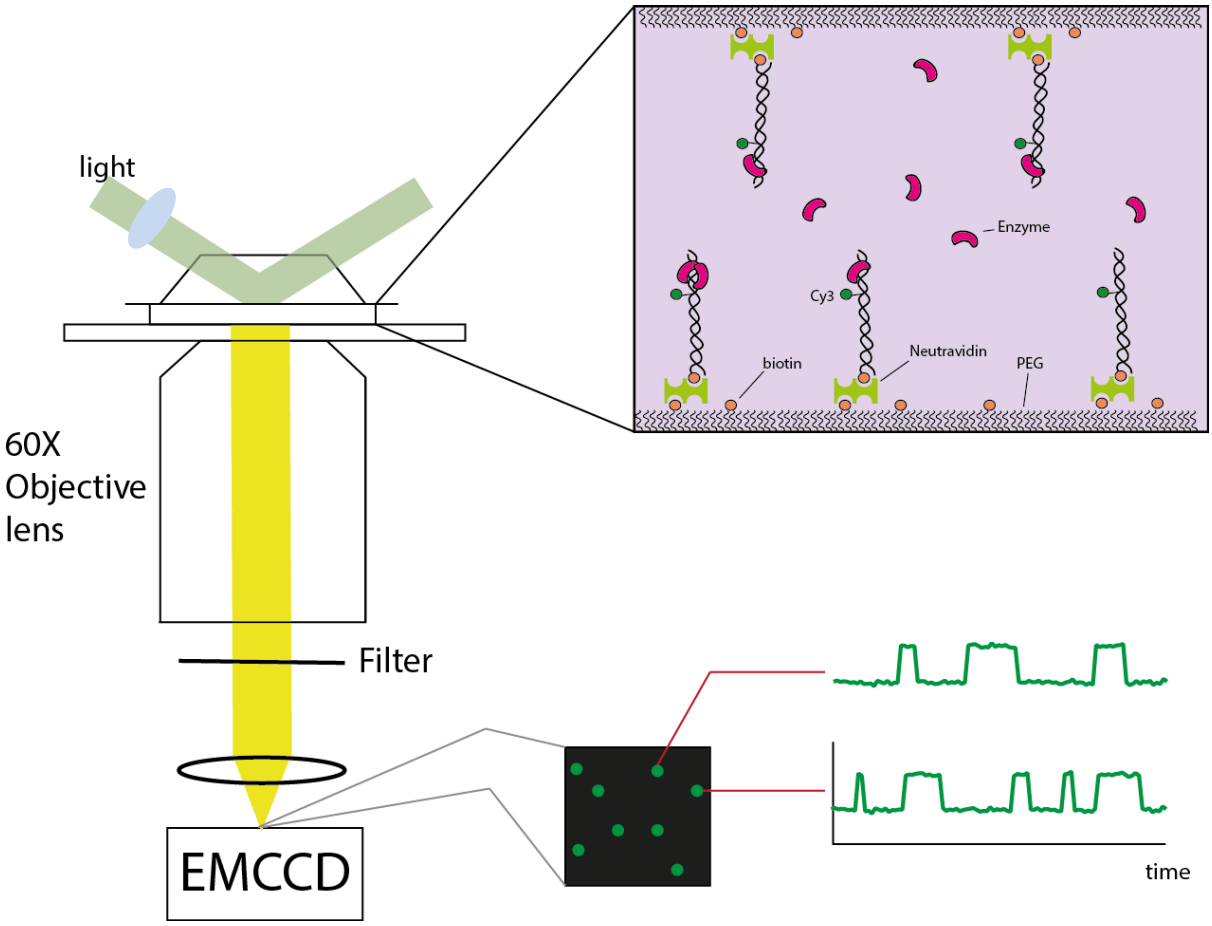

Figure 2. Prism type TIR: incident light with greater than the critical angle creates total internal reflection, and induces evanescent field. The molecules immobilized on the surface of a quartz are excited by evanescent field. Individual molecules can be tracked.

2.2 Protein binding induced fluorescence

Helen Hwang et al. addressed that the fluorescence dyes which bear *cis-trans* isomerization have protein binding induced fluorescence, PIFE, effect.[3] Fluorescence of *cis-trans* isomerizable dyes including Cy3 and Cy5 are enhanced by protein binding nearby and this property has been used in stopped-flow.[4] The mechanism of PIFE is not elucidated yet, but it is often used to observe the kinetics of a molecule. In this study, Cy3 was labeled 3bp far from the *Hin*dIII recognition site. The PIFE effect stated by Hwang was examined with the fluorophore labeled on the base of the oligonucleotides. Similar PIFE effect was observed with the fluorescence dye labeled on the backbone of DNA oligonucleotides. The PIFE effect that is address in this study is all based on the interaction between the protein and DNA with Cy3 labeled on a backbone. Protein association on dsDNA with Cy3 labeled nearby induces the fluorescence enhancement and dissociation decreases the fluorescence.

Fluorescence Resonance Energy Transfer, FRET, is a convenient technique to study the dynamics and kinetics of molecules. However, labeling fluorophores on a protein or DNA is inefficient and time consuming. Also, FRET is limited to its pair that energy can be transferred from a donor to an acceptor. FRET is useful when the conformational change or dynamics occur between 3-8 nm.[5] On the other hand, employing the photophysical property of an isomerizable fluorophore such as Cy3 to study the kinetics of molecules has great advance in easy preparation. A complicated protein labeling and FRET pair are not required. For certain enzymes, fluorescence intensity library exists with base pair sensitivity.[3]

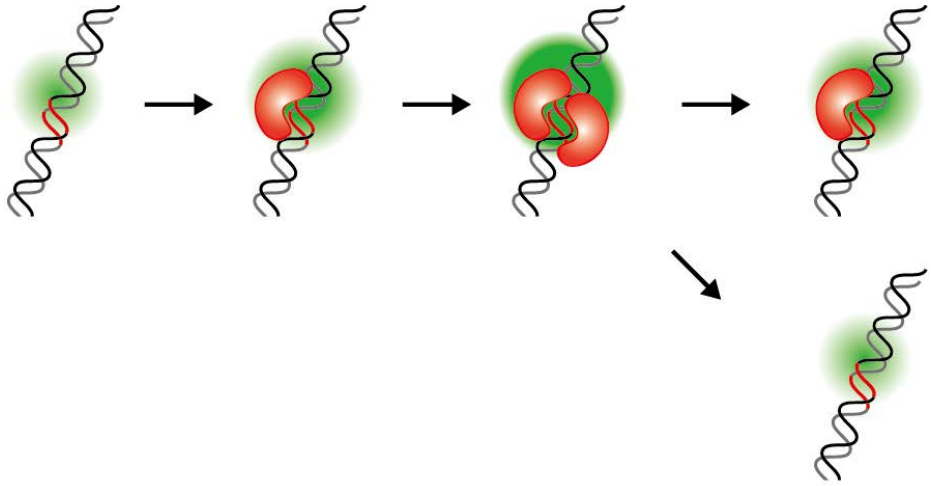

Figure 3. Scheme of protein induced fluorescence enhancement. The green area indicates the Cy3 labeling, and the red lines on the DNA indicates the specific site that the enzyme binds.

2.3 Restriction endonuclease, *Hin*dIII

*Hin*dIII is a type II restriction endonuclease which recognizes 4-8 specific sequence and cleaves the binding site with a cofactor Mg^{2+} ion.[6] *Hin*dIII recognizes and cleaves the palindromic sequence 5'-A/AGCTT-3'.[7] *Hin*dIII is comprised of 300 amino acids and has a molecular weight of 34.950 kDa.[8]

*Hin*dIII is a homodimer which activates its nuclease activity when two proteins compose a dimer along with the DNA. Figure 4 shows the crystal structure of *Hin*dIII endonuclease. Each red and blue chain is a single *Hin*dIII protein. They bind to the recognition site and cleave the site. The fundamental reaction mechanism of restriction endonucleases is known as hydrolysis of the phosphodiester backbone of DNA.[6, 9]

There were several standards to be satisfied for studying the effects of methylation to DNA and protein interactions. First, commercial enzyme must be available. Second, binding sequence should be well known. Third, the size should not be too big because its interaction with DNA can be disturbed by the fluorophore and difficult to observe the kinetics by TIRF. At last, the recognition sequence should have at least one cytosine for methylation because in prokaryotic and eukaryotic genes,

methylation occurs mostly at cytosine.[10] *Hin*dIII was appropriate for study of effects of methylation with the identified binding site and cytosine of the site (AAGCTT) that can be methylated. *Hin*dIII with 100,000 U/ml was purchased by New England Biolabs.

Mg^{2+} is a cofactor that binds between the DNA and protein and promotes the hydrolysis of the phosphodiester bond by water and cleaves the recognition site of *Hin*d III. Mg^{2+} ion can be replaced by other metal ions such as Mn^{2+} and Ca^{2+}. Several other divalent ions were tested for cleavage activity and the result that Ca^{2+} has the less cleavage activity coincide with the previous report by D.Tang.[11]

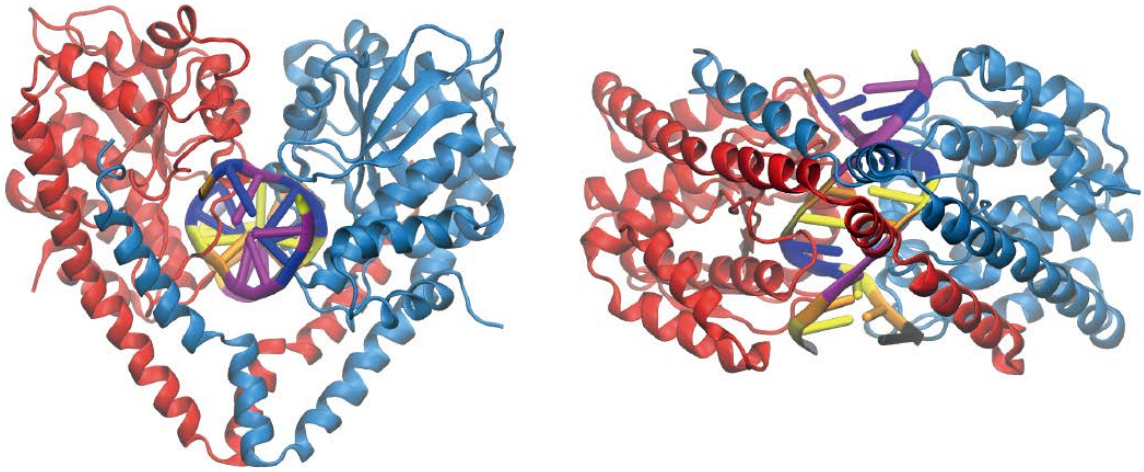

Figure 4. Structure of *Hin*d III. (Left) upper view, and (right) side view

2.4 Sample Preparation

DNA oligonucleotides

The following oligonucleotides (shown 5'-3') were used (manufactured by IDT DNA): GAATGCACGCATGCATCGATAAGCTTCGATCGATAGAAAAAAAAAAAAAAAAAAAAAA AAAAAAA (wild type complement strand), Biotin- TTTTTTTTTTTTTTTTTTTTTTTTTTTTT, TATTCGAAGC/iCy3/TAGCTATC (Cy3 labeled strand), GAATGCACGCATGCATCGATAAG/iMe-dC/TTCGATCGATAGAAAAAAAAAAAAAAAAAAAAAAAAAAAAA (Methylated complement strand), GAATGCACGCATGCATCGATAAATTTCGATCGATAGAAAAAAAAAAA AAAAAAAAAAAAAAAAAAA (NonSpecific complement). The oligonucleotides were PAGE purified when longer than 60 base pair, otherwise they were HPLC purified.

Quartz modification

The quartz (Prism Research Glass, Inc) were coated with polyethylene glycol, PEG, following the protocol from "**Single-molecule Techniques:** A Laboratory Manual" by Paul R. Selvin and Taekjip Ha. On the surface of an aminoxylane modified quartz, m-PEG (Laysan Bio) and biotin-PEG (Laysan Bio) are spread with 80:1 ratio. 0.1 mg/ml neutravidin is added on the surface of a quartz and incubated for 10 minutes.[12] Neutravidin is applied on a surface to immobilize the biotylated DNA substrates. The substrate is biotylated at 5' end, and Cy3 dye labeled in the middle with NHS ester link. About 20 pM of the substrates are applied on top of the surface, and incubated for 10 minutes. DNA substrates are immobilized on the quartz through neutravidin-biotin interaction. The surface of a quartz is then washed with T50 buffer (10mM Tris-HCl pH 8, 50 mM NaCl). Imaging Buffer, IB, is required to visualize the fluorophores. IB contains Tris pH 8 (0.1 M), Trolox ((±)-6-Hydroxy-2,5,7,8-tetra-methylchromane-2-carboxylic acid; Fuka)[12], NaCl, DTT, Bovine serum albumin (BSA; New England Biolabs), T50, glucose, and Pyranose oxidase from Coriolus sp.(Sigma-Aldrich).

The fluorophore labeled substrates are immobilized on a surface of a quartz through biotin-neutravidin interaction. Right after IB is applied on a surface with the substrates, place the quartz on an objective lens and view the molecules.

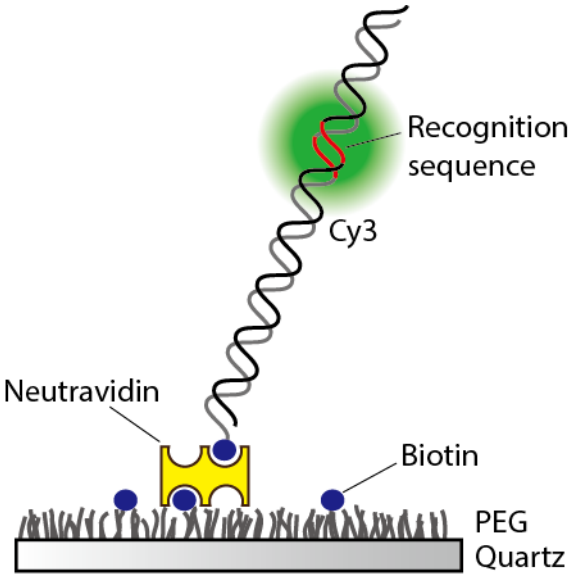

Figure 5. Immobilized dsDNA substrate on a PEG-coated quartz through biotin-neutravidin interaction. Recognition sequence is indicated in red, and the Cy3 fluorophore as a green area over the sequence.

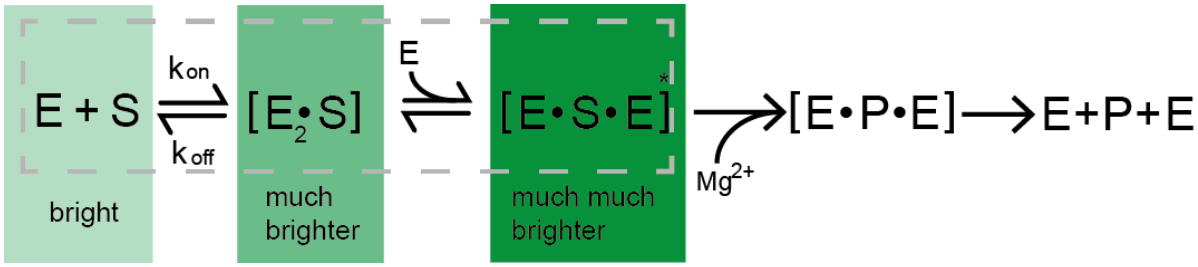

Figure 6. Expected reaction flow scheme.

3. A Novel way of detecting the protein association and dissociation dynamics and the dimer formation of a protein

3.1 Introduction

Understanding the dynamics of proteins comprises much information of protein-protein and protein-DNA interaction. Furthermore, understanding dynamics of a single protein can determine the hidden steps which were not observed in bulk material, and elucidate the interactions more accurately.

The association and dissociation dynamics of a restriction endonuclease *Hin*dIII was observed at a single-molecule level with TIRF. Each association and dissociation rate was determined. Transient state of conformational change followed by the association of the protein was observed with PIFE effect as well.

We report that kinetics of a protein can be studied with a fluorescence assay at a molecular level. Reaction rate such as association and dissociation rates were determined by the single molecule kinetics study.

*Hin*dIII is known as homodimer which requires two units of protein to have a catalytic activity. The reaction was expected as figure 6. E indicates *Hin*dIII restriction endonuclease, S as DNA substrate, and P as products which are cleaved. Enzymes associate with the DNA substrate that has specific binding sequence, and as enzyme binds to the substrate, the fluorescence of Cy3 is increased by PIFE effect. Enzyme and substrate complex itself is inefficient in enzyme activity, but when a *Hin*dIII dimer is formed, it is completely bound to the substrate and the conformational change which increases the fluorescence by tighter complex occurs.

3.2 Experimental

3.2.1 Fluorescence enhancement

The biotylated DNA substrate with *Hin*dIII binding sequence was first incubated with *Hin*dIII enzyme to confirm whether the fluorescence is enhanced when cis-trans isomerizable dye Cy3 is labeled in the vicinity of the protein binding sequence. Figure 7 shows wild type sequence and the distance between the Cy3 fluorophore and the recognition. As type II restriction endonuclease, the recognition site is in which the enzyme binds to. In order to find the optimal nucleic acid labeled to have the brightest intensity when a protein binds, we labeled Cy3 at different bases. From one base far from the recognition site (AAGCTT) to the tail of the DNA, Cy3 was labeled at various bases and tested for the optimal condition for PIFE effect. When Cy3 was labeled right next to the recognition site, the Cy3 signal was not enhanced with the enzyme, and it can be assumed that Cy3 fluorescent molecule disturbed the binding of a protein. On the opposite side, when Cy3 was labeled at the tail of the DNA, the PIFE effect could not be observed enough to analyze. The enhancement was subtle, and finally the optimal position was in which 3 bases far from the recognition site.

The figure 8 shows that the enzyme, *Hin*dIII, injection increased the fluorescence in ensemble. It was measured with a fluorometer in imaging buffer. The buffer with DNA substrates have an emission fluorescence of Cy3 at around 560 nm, and after the injection of enzyme in buffer, the intensity of the fluorescence increased. The green area indicates the increased amount of fluorescence. The phenomenon of fluorescence intensity increment through protein injection was also confirmed as protein binding at a single-molecule level by TIRF. In figure 9, the panel on the right side is a view of EMCCD. Each white spot indicates fluorophore of a molecule immobilized on a quartz surface. When the dsDNA with enzyme specific binding sequence are incubated with enzyme, the white spots became much brighter. The upper view without the enzyme contrasts from the one below. The view with the enzyme definitely shows brighter fluorescence. In figure 9, the single exponential graph of Gaussian function was changed to the bimodal distribution with the injection of the enzymes.

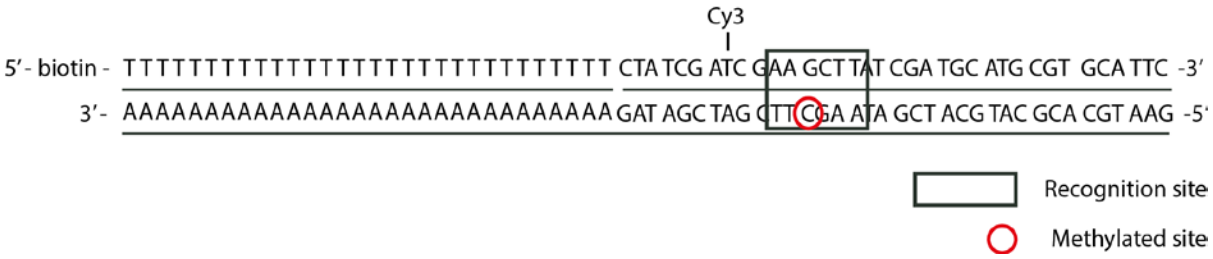

Figure 7. Sequence of dsDNA. The recognition site of *Hin*dIII is AAGCTT. Cy3 fluorescent is labeled three bases far from the sequence. For the methylated sequence, the cytosine in the middle of the recognition site opposite to Cy3.

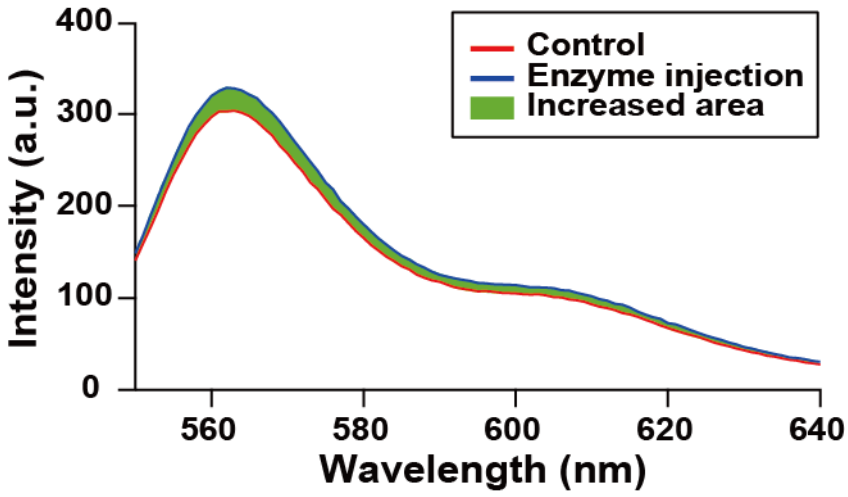

Figure 8. PIFE effect in ensemble. Increased fluorescence after enzyme (*Hin*dIII) injection was measured by fluorometer

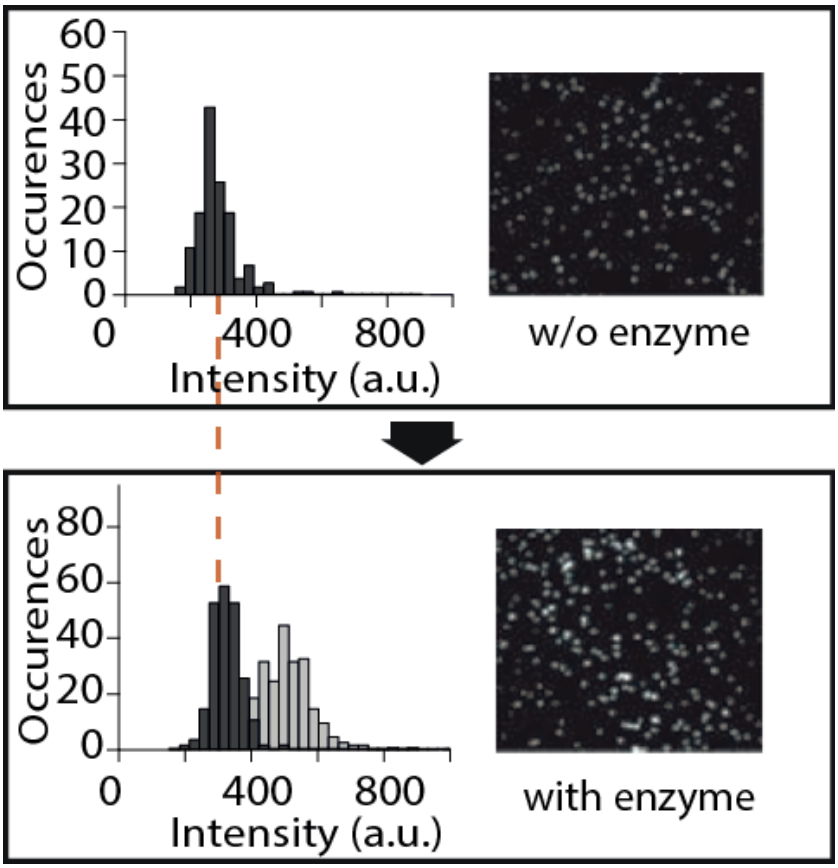

Figure 9. PIFE effect in single-molecule. (Upper) Wide-field images before the *Hin*dIII injection, and histograms of fluorescence intensities. (Below) After the enzyme injection, the fluorescence function was changed to the bimodal function.

3.2.2 Kinetic analysis of association and dissociation

The figure 10 is a scheme of DNA and protein interaction at TIRF. The DNA substrates are immobilized on a surface of a quartz by biotin-neutravidin interaction. The DNA substrates are labeled with Cy3 near the binding sequence of *Hin*dIII. While proteins are repeating the association and dissociation with the divalent ion, Ca^{2+}, k_{on} and $k_{off,}$ which indicate the rate of association and dissociation respectively, are calculated. Applying PIFE effect, TIR is utilized to give a fluorescence trajectory of a single molecule which increases the fluorescence as the protein binds near the Cy3 where recognition site exists.

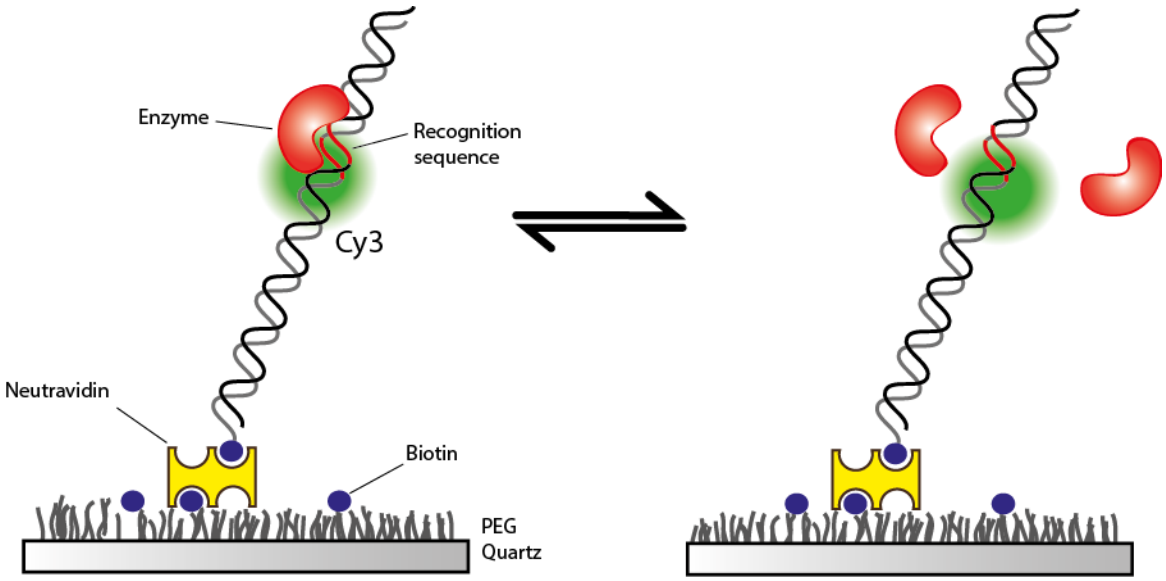

Figure 10. Single-molecule scheme of DNA and enzyme interaction on a substrate-immobilized quartz.

3.3 Results and Discussion

3.3.1 Reaction time in ensemble

Prior to the single-molecule test, the reaction time should be measured and confirmed that it is short enough to be observed at a single-molecule level. 2 μM dsDNA was incubated with the reaction buffer (buffer condition is indicated in figure11) for 1, 5, 10, 20, 30 and 40 minutes and the reaction was quenched by adding EDTA (0.4 M final). The fraction ratio is correlated to the enzyme activity, and shows how fast the reaction is. The catalytic rate, or also called the turn-over rate, K_{cat} of *Hin*dIII is 9.53 x 10^2/min.[11] In figure 11, after 20 minutes, over 80% of fractions were produce confirming that the reaction is fast enough to be tested at a single-molecule.

3.3.2 Enzyme concentration

Concentration of enzyme varied from 1 to 5 nM, while concentration of substrate dsDNA was about 1.2 μM. The fraction ratio was proportional to the concentration of enzyme, and showed the linear fit.

3.3.3 Specific vs. Nonspecific binding

We prepared dsDNA containing *Hin*dIII recognition sequence (AAGCTT, wild type, WT), and non-recognition sequence (AAATTT, NonSeq). Figure 18 (A) is a three different sets of sequence; Wild Type, Methylated sequence, and sequence without the recognition site. HPLC-purified sample was Cy3-labeled at 3 bps far away from the recognition site. Using agarose gel analysis, we tested the catalytic activities and reaction rates of each oligonucleotide in the presence of Mg^{2+}. After 30 min incubation at 37 °C, as shown in figure 18 (B), we found that NonSeq has no activity with *Hin*dIII, showing that the concentration of enzyme in the experiment does not show any significant nonspecific catalytic reaction.

Non-specific strands are known to have different conformations from wild-type dsDNA that inhibits the DNA hydrolysis. In case of *Eco*RV of which is another restriction endonuclease from family of Type II restriction enzyme, the non-specific strand is not distorted enough for magnesium ion to be bound to the substrate and catalyze. A similar assumption can be made for *Hin*dIII.[13]

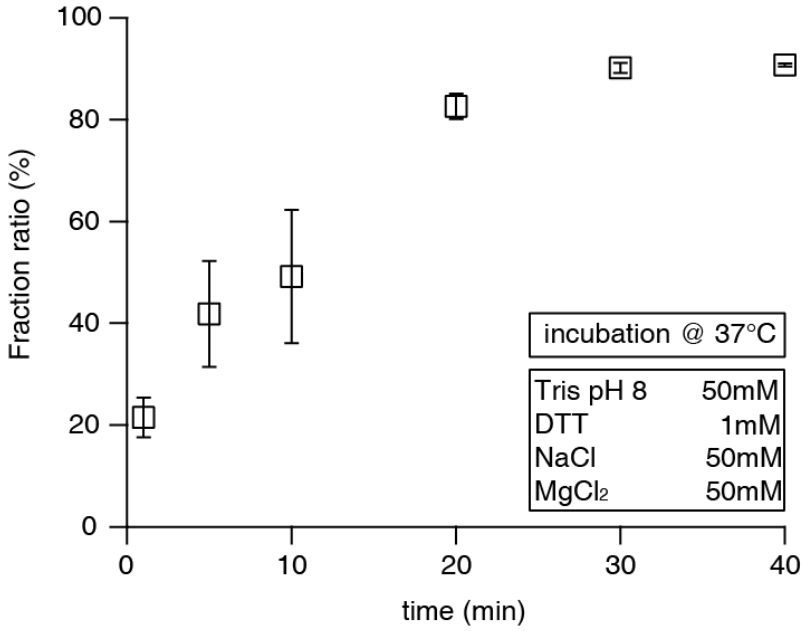

Figure 11. Enzyme activity as a function of time.

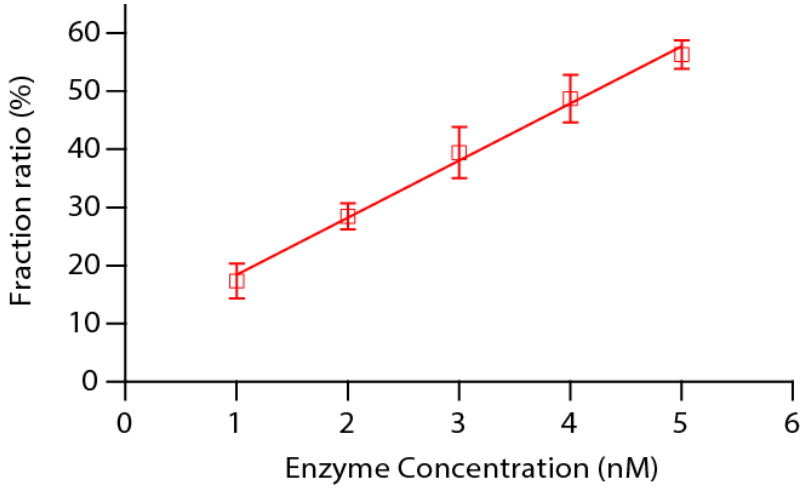

Figure 12. Enzyme activity as a function of enzyme concentration.

3.3.4 Single-molecule test

3-State Kinetics

Figure 13 is a representative data that shows the trace that was obtained for more than 60 seconds and fitted with Hidden Markov Model (HMM). Three transient steps indicate each association and dissociation steps. The lowest state (S1) is the unbound state, the second state (S2) is the first enzyme bound state, and the third state (S3) is when two enzymes are bound to the sequence and results the conformational change. To acquire the trace, Ca^{2+} was used in place of Mg^{2+} because Mg^{2+} functions as a cofactor and cleaves the sequence while Ca^{2+} still helps association of the enzyme but does not cleave the DNA. Enzyme injection causes a repetitive fluctuation of fluorescence. The intensities of the fluctuation seem rather constant. The higher level duration and the lower level duration of many single molecules are represented as a function of occurrences and fitted with exponential decay function: F(t) = Ae^{-kt}.

k is a variable indicating the reaction rate constant. When *k* value increases, the duration is shorter, and vice versa. k_1 is an association rate constant of enzyme, and k_{-1} is a dissociation rate constant and k_{-2} is a rate constant of conformational change refer to the reaction flow figure 6. In figure 14, we collected all the date of a single molecule, and measured the each duration time of S1, S2, and S3 which are related to association, dissociation and conformational change, respectively. The histograms were fitted with single exponential decay function.

Another state S3 is the time duration of conformational change. *Hin*dIII is known as homodimer, and it does not have its nuclease activity unless it forms a dimer. After the proteins are dimerized, they bind to the substrate which later kinks the DNA. *Eco*RV, type II restriction endonuclease, dimerizes and kinks the DNA to ~50° in the presence of metal ion.[14] It is known that *Hin*dIII also kinks the DNA, and distorted when bound with a metal ion.[7] The S3 can be elucidated as another fluorescence enhancement by distortion of DNA.

Enhancement factor of first and the second increment was calculated. The first enhancement factor of S2 state was 1.6, and that of S3 was 1.9. Figure 15 represents the fluorescence intensity increment factor of four different concentrations. The bimodal distribution diagram represents the S1 and S2 states, and the fluorescence enhancement factor is 1.6 at all concentrations. The rate of S3 is too fast having a transient life time that it was not clearly observed in these distributions. When enzyme concentration increases, the association rate (S1) increases as well, which means the higher population of enzyme has a higher possibility of colliding and eventually binding to the DNA. The dissociation rate (S2) was constant that the dissociation rate does not depend on the enzyme concentration.

The enzyme concentration did not influence the intensity ratio between lower and higher level. As it is shown in figure 16, at various enzyme concentrations the ratio between the lower and the higher fluorescence was equal to 1.6.

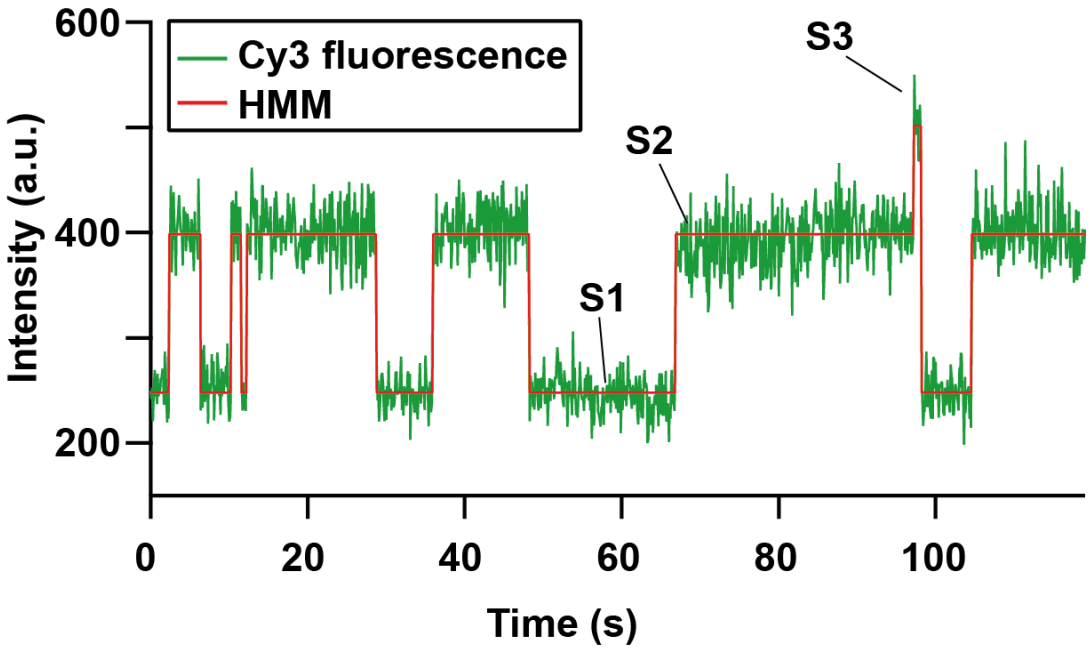

Figure 13. A representative single-molecule fluorescence trajectory. When *Hin*dIII is injected, Cy3 fluorescence on DNA is fluctuating

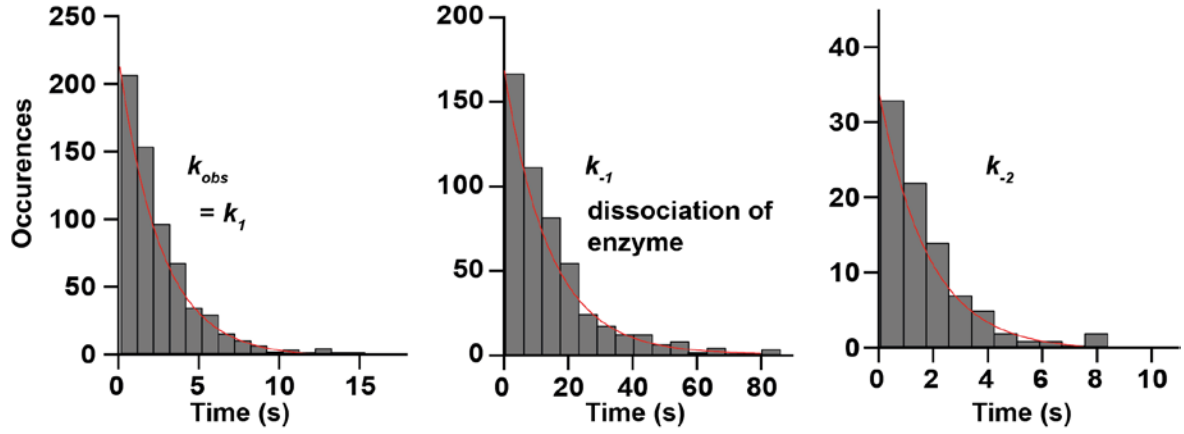

Figure 14. Kinetic analysis for determining rate constants of each reaction step. Example of histograms of the duration times of each reaction step. Histograms were fitted to a single exponential decay curve (red curve).

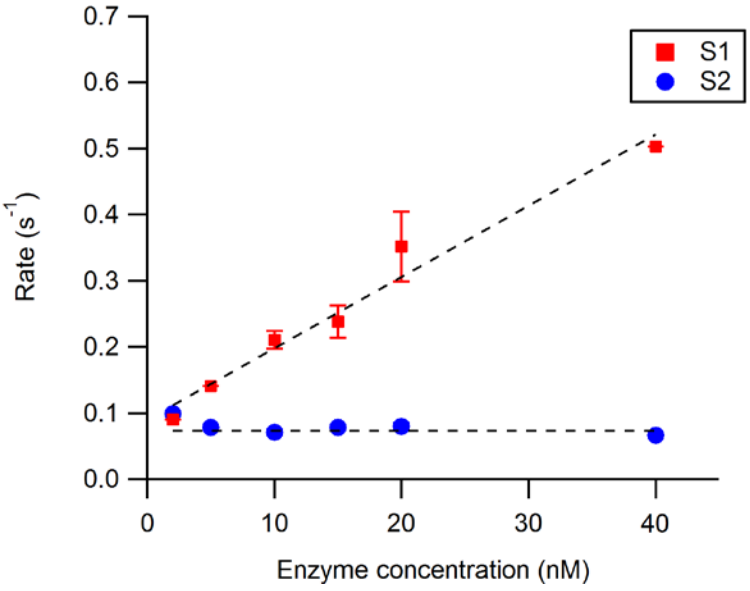

Figure 15. Rate of lower and higher level of fluorescence as enzyme concentration varies. S1 state is a enzyme unbound state, and S2 is a bound state.

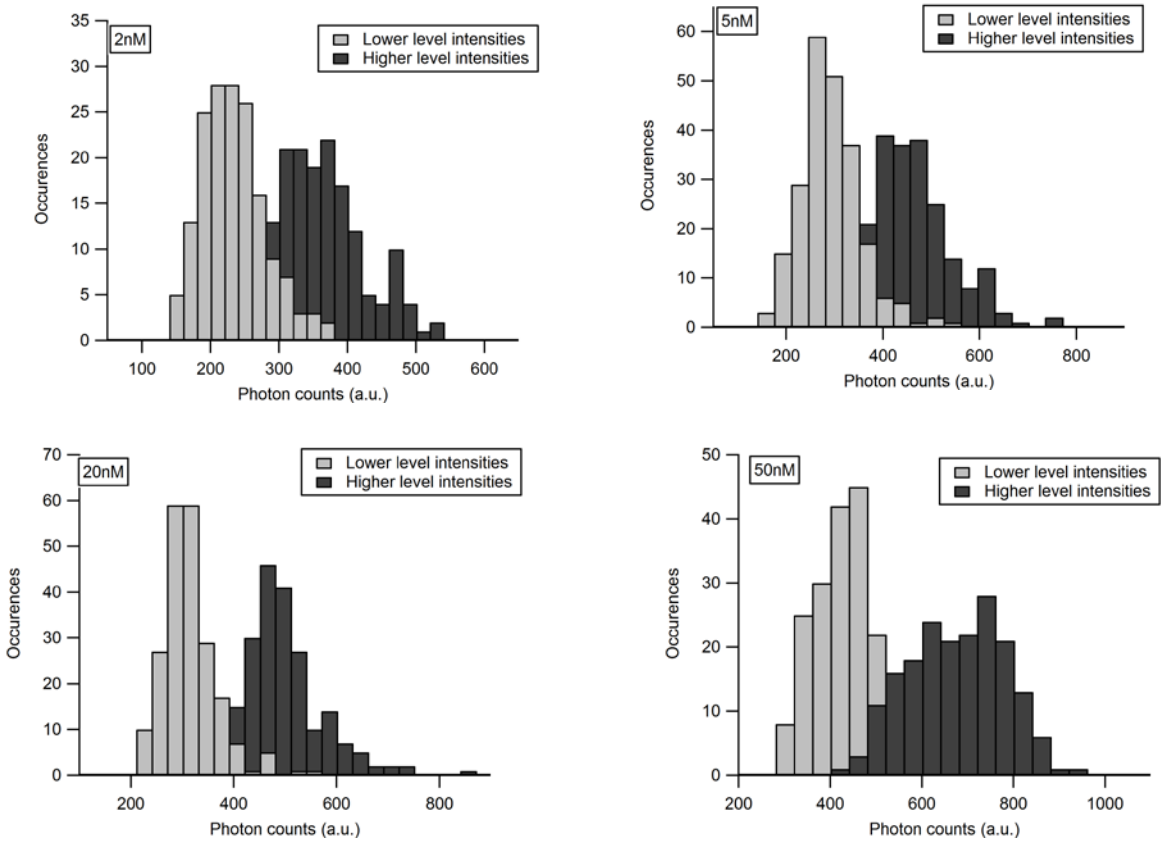

Figure 16. Fluorescence intensity at 2 nM, 5 nM, 20 nM and 50 nM.

Population ratio and equilibrium constant state

Among the rate constants of each reaction step, the measurement of nuclease conformational change rate constant k_2 is so slow that we cannot acquire enough numbers of individual molecules for statics with the conventional single-molecule setup and fluorophores. In order to obtain its value, we introduced the relationship between the equilibrium constant and the concentration of molecules. Now, we consider the chemical equation based on Michaelis-Mentens equation. At equilibrium, the relationship of each chemical reaction rate can be expressed as $k_{on}\cdot[E]\cdot[S] = k_{off}\cdot[E\cdot S]$. We note that if $[E]>>[S]$, the ratio of the concentration ($[E\cdot S]/[S]$) at equilibrium equals the value for $[E]\cdot(k_{on}/k_{off})$. To test the suitability of this kinetic analysis, we compared the ratio of the population (P_{S2}/P_{S1}) and the equilibrium constant (k_{-1}/k_1) of the reaction. As shown in figure 17 (B), we observed similar linear plot. Next, we carried out this analysis to reveal conformational change rate constant k_2.

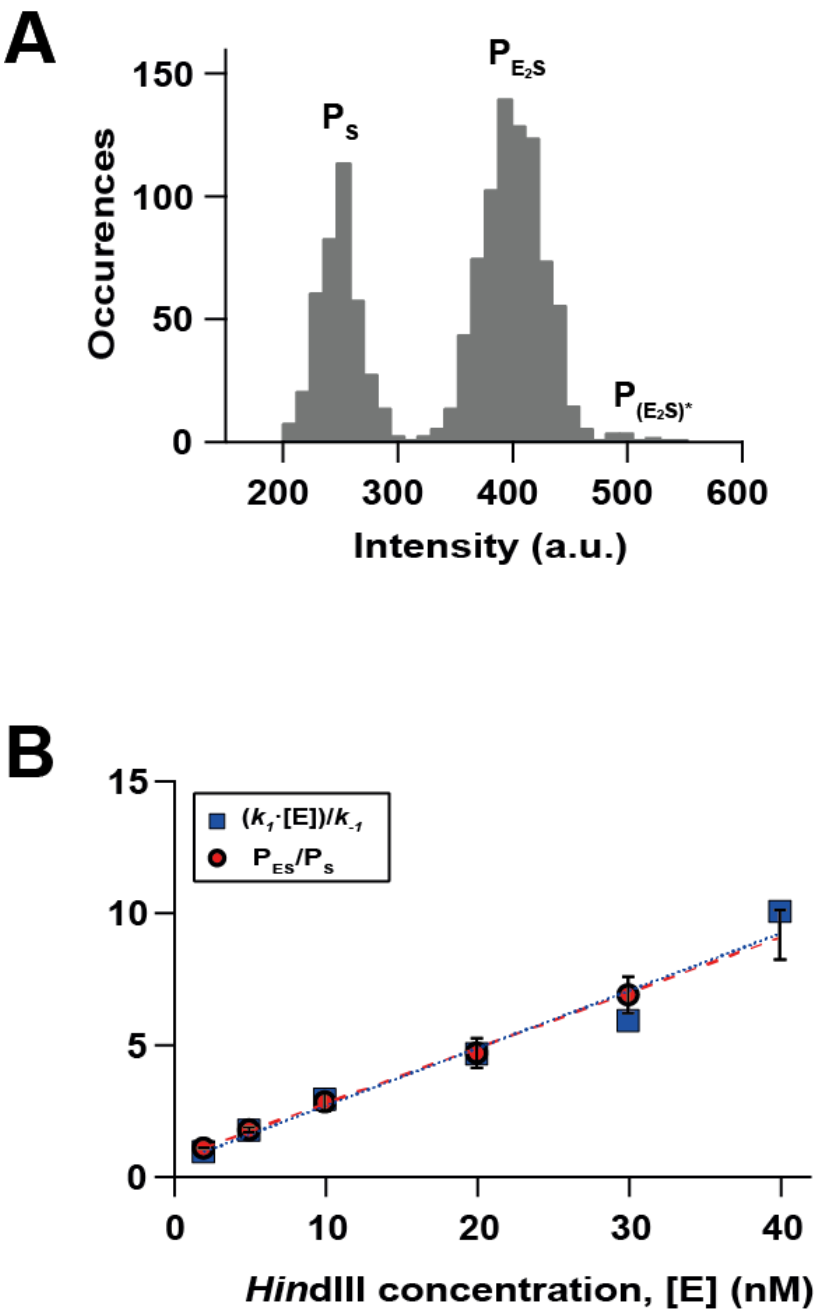

Figure 17. (A) population graph of each state. P_s, P_{ES}, P_{E_2S} are from S1, S2, and S3 state respectively. (B) The population ratio of P_{ES}/P_S.

3.4 Conclusions

First, the kinetics of association and dissociation of *Hin*dIII on DNA was observed by single-molecule technique, TIRF using PIFE effect. The samples were designed to have the most optimal condition to show PIFE effect. By PIFE effect, the fluorescence fluctuates as interacting with the enzymes. The analysis of duration time of high and low level of fluorescence intensity fluctuation was calculated to obtain the association and dissociation rate constants. Thus, the third step of conformational change followed after dimerization was observed.

The optimal conditions for enzyme kinetics were concerned including ion concentration, enzyme concentration, buffer condition, and non-specific binding control tests.

4. Effects of methylation on dsDNA to dissociation protein from dsDNA.

4.1 Introduction

In prokaryotes, native DNA is preserved by methylation. When foreign genes from a bacteriophages are transferred to a prokaryote, methylation of DNA can be a defense against the foreign DNA to keep their native genes.[15] Methylation behaves as a marker that reports not to cleave its native dsDNA. In the meantime, foreign dsDNA are cleaved by restriction endonuclease. Methylation in eukaryotic cells are also closely related to gene regulation and gene expression.[16] Many studies have been done about the effects of methylation but it is still a subject for intense research at a molecular level.

Cytosine of a recognition site (AAGCTT) was hemi- methylated from IDT DNA. Nuclease activity of restriction endonuclease, *Hin*dIII, was tested in ensemble and compared with the wild type (non-methylated), and dsDNA with non-recognition sequence which does not involve specific binding. Through agarose gel result, it was confirmed that when a specific binding sequence is point mutated, protein does not show a nuclease activity, and methylated sequence shows ~10 % less activity efficiency (Figure 18 (B)). When both strands of DNA are methylated at cytosine, there is no nuclease activity (data not shown).

4.2 Results and Discussion

4.2.1. Ensemble test

The enzyme activity was tested with three different substrates: wild type, hemi-methylated, and non-specific sequence DNA. The wild type includes the specific binding site of *Hin*dIII, and the full sequence is in figure 18 (A). The hemi-methylated sequence has a functional group of methyl at the cytosine of the specific binding site. The non-specific sequence DNA has a sequence that does not include the binding site (AAGCTT). The activity of three substrates were tested with an agarose gel, 2 μM DNA were diluted in buffer containing 50 mM of Mg^{2+}, and ~35 nM *Hin*dIII enzyme was added and incubated for 20 min at 37 °C. As a consequence, the fraction ratio which is correlated to the activity of the enzyme reaches over 80% in the case of WT (wild type), and around 70% (hemi-methylated) and almost 0% for the non-specific sequence. It has been confirmed that the non-specific sequence DNA does not show any enzyme activity.

The activity time was also compared between the wild-type and the hemi-methylated type. The reaction condition was the same except, the reaction was stopped by EDTA for every 1 min, 5 min, 10 min, 20 min, 30 min and 40 minuites. The results were clearly distinguishable between two substrates. The wild-type was saturated faster than the methylated one (Figure 18 (C)).

Another control test done to prepare the single-molecule experiment was to confirm that the labeled Cy3 fluorescent dye does not affect the restriction endonuclease activities (Appendix). It was also tested in the same reaction buffer at 37 °C for 20 minutes and clarifies that there is no great difference in the activity between the labeled DNA and non-labeled DNA.

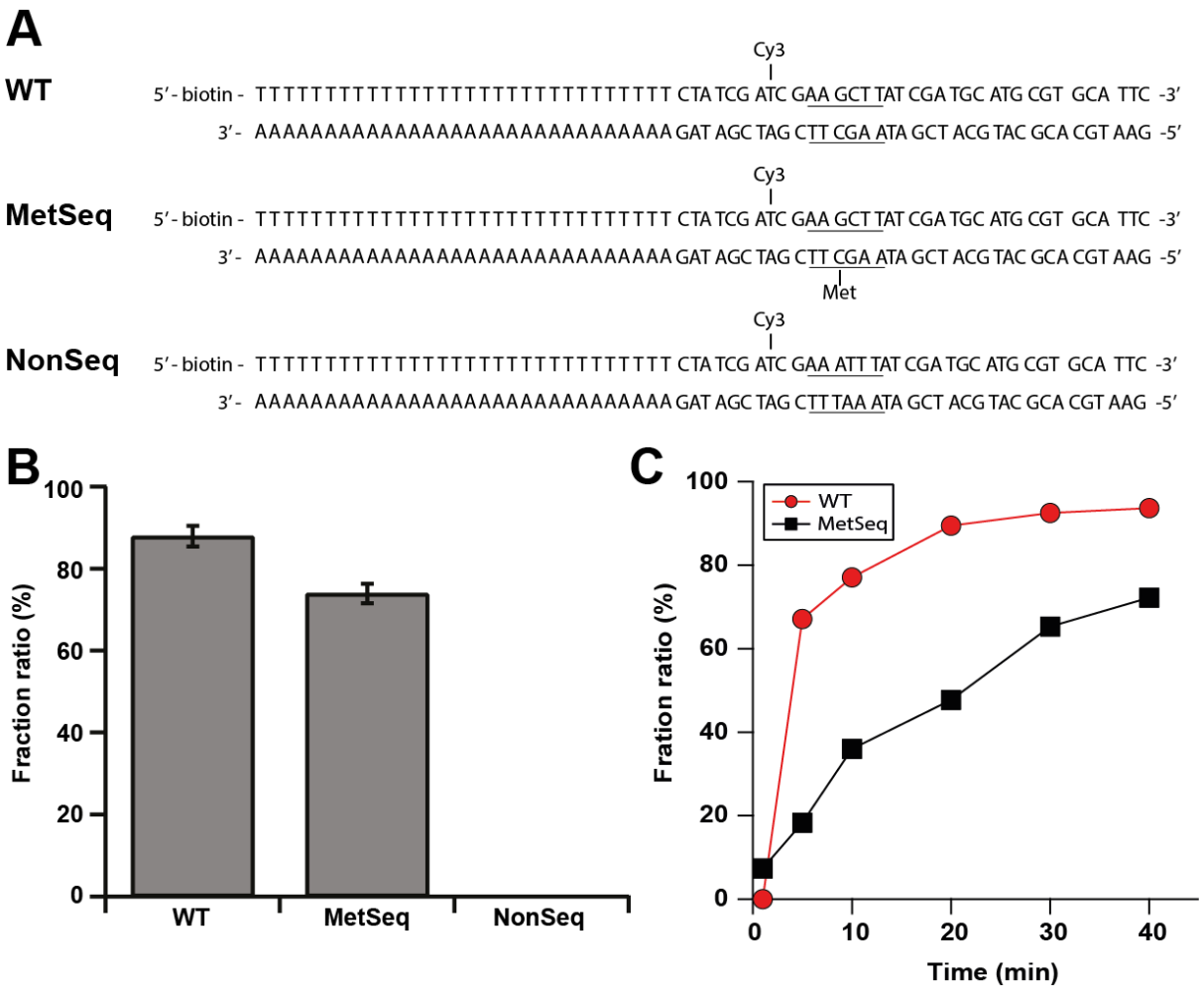

Figure 18. Kinetic difference between WT and MetSeq during the enzymatic catalytic reaction of *Hin*dIII. (A) All oligonucleotide sequences that we used in ensemble and single-molecule measurements. On three oligonucleotides, Cy3 is labeled on the proximal position (3 bps) of *Hin*dIII recognition sequence and biotin is covalently attached on 5' end for immobilizing on the quartz slide. In addition, 5-methylcytosine (5 mC) substituted for a cytosine on the recognition sequence in MetSeq. (B) Ensemble measurement for the enzymatic rate on WT and MetSeq (2 μM) in the presence of 30 nM *Hin*dIII at 37 °C. The catalytic rate of each oligonucleotides can be obtained by fitting with a function, $F(t) = A \cdot (1-\exp(-k \cdot t))$. The k value for WT is 0.194 min^{-1}, and the *k* value for MetSeq is 0.051 min^{-1} (left panel). For 40 min incubation at 37 °C, the cleaved product with MetSeq is ~10 % lower than the product with WT (right panel).

4.2.2. Single-molecule test

We tested three types of methylated DNA substrates: methylated on the both strands on the binding site, hemi-methylated on the Cy3 labeled strand, hemi-methylated on the opposite of the Cy3 labeled strand. The DNA substrate with both strands methylated did not show an activity, but the both hemi-methylated substrates showed a subtle difference in equilibrium constant compared to the methylated type.

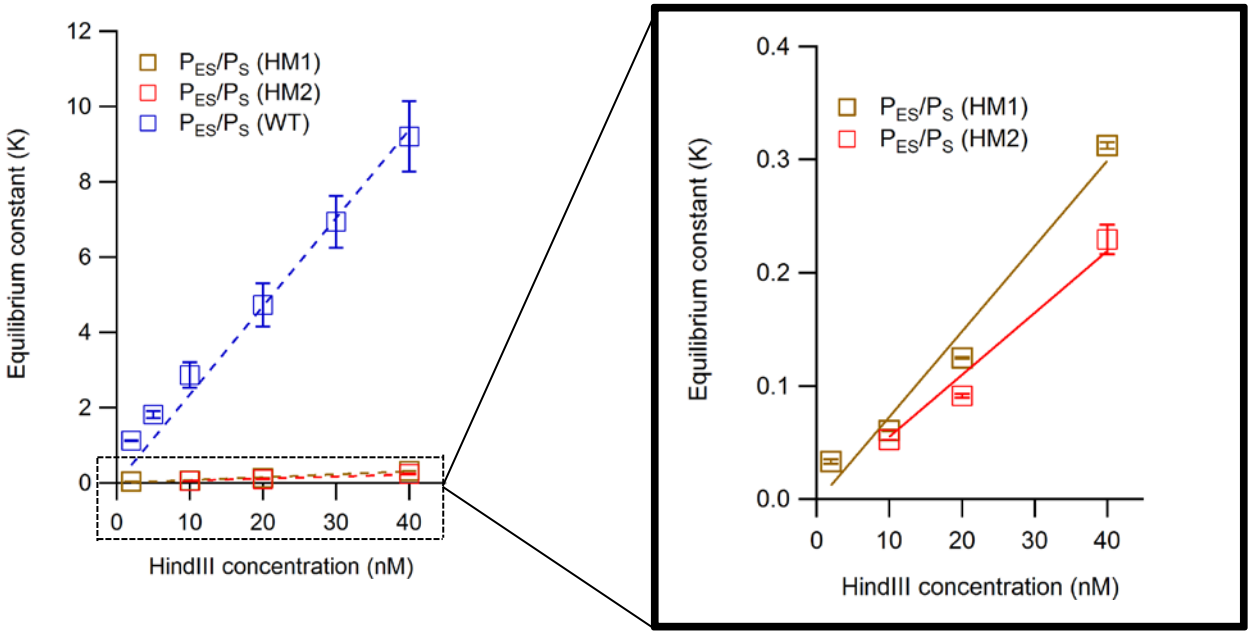

Figure 19. Kinetics comparison between two hemi-methylated substrates. The population ratio from P_{ES} to P_S of hemi-methylated substrate 1 (HM1) and hemi-methylated substrate 2 (HM2) has a small difference, while the wild-type (WT) has a greater equilibrium constant which infers the greater enzyme activity.

The results of protein kinetics against the wild-type DNA and hemi-methylated DNA were utterly different. As shown in figure 19, the wild type DNA and methylated DNA show a main difference in the duration of binding. The binding rates are similar whereas the dissociation rate was much greater in methylated sequence DNA. The duration time of enzyme binding of WT strand with 20 nM at 310 K is about 13.81597, and the duration time of enzyme binding of methylated sequence is about 0.34825. Figure 20 is the representative trace of each wild-type and methylated type substrate. The duration time of bound state has decreased rapidly. The duration time of unbound state was almost the

same as shown in figure 22 (B). The fluorescence enhancement factor was the same as 1.6 as it was observed with WT (Figure 22 (A)). In all experiments, Ca^{2+} was substituted for Mg^{2+} to prevent cleaving.

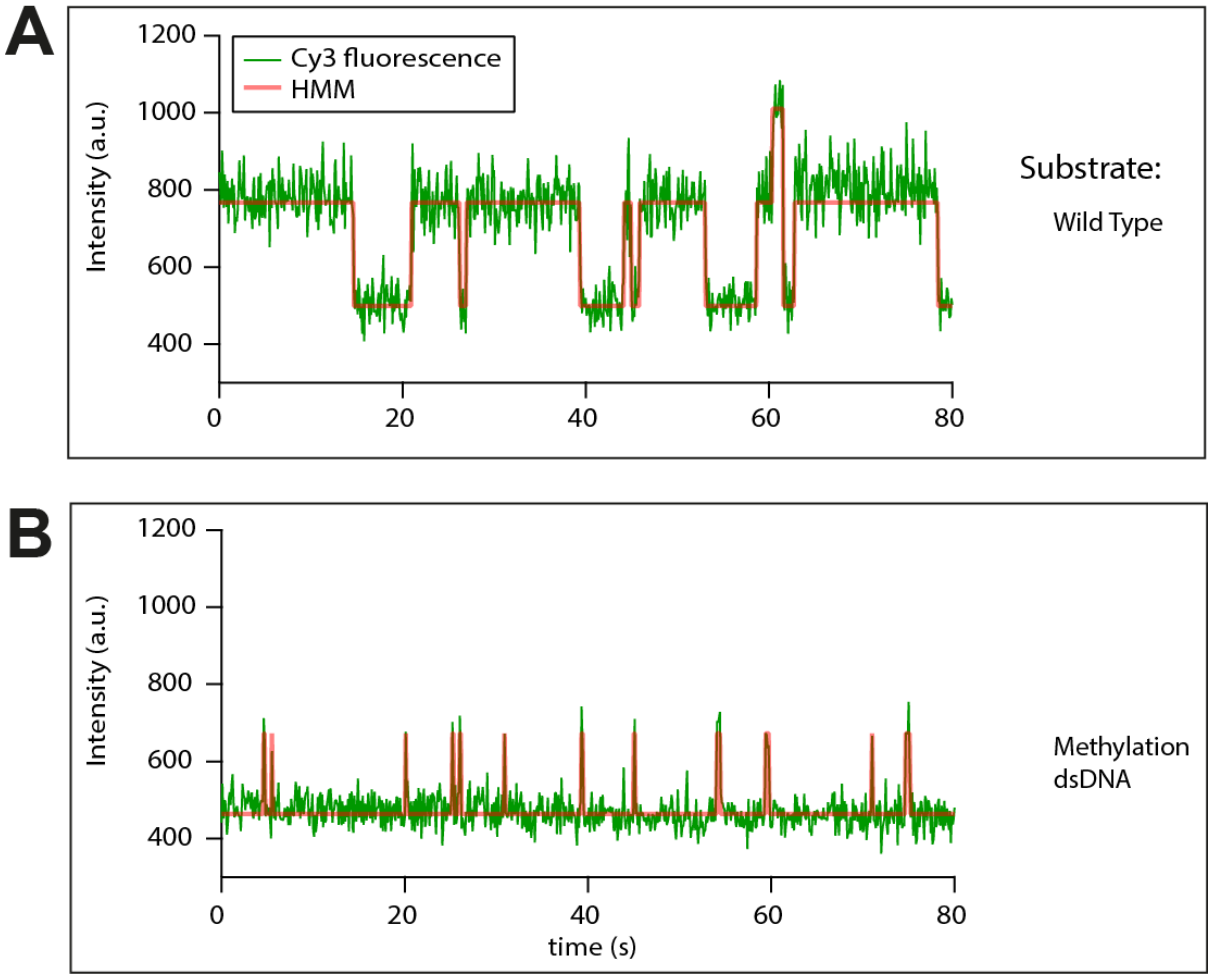

Figure 20. A trajectory of a single molecule. (A) Trace of a Cy3-labeled DNA substrate with *Hin*dIII. The fluorescence is enhanced from 500 a. u. to 800 a.u. The enhanced duration indicates the protein binding in the protein-recognition site. The lower level fluorescence indicates the dissociated duration. (B) Trace of a Cy3-labeled DNA with methylated cytosine in the recognition site. The trace shows a short duration time of the binding of a protein.

4.2.3. Arrhenius plot

Single molecule experiments were repeated in different temperatures; 25, 26, 30, 34, 37 ˚C to understand the thermodynamic properties of the reaction. From the Arrhenius equation (below), the ln *k* vs.1/T plot can be drawn and the activation energy can be calculated from the slope.

$\ln k = \frac{-Ea}{R}\frac{1}{T} + \ln(A)$

k: rate constant, E_a: activation energy, R: Gas constant, T: temperature, A: frequency factor (total number of collisions per second)

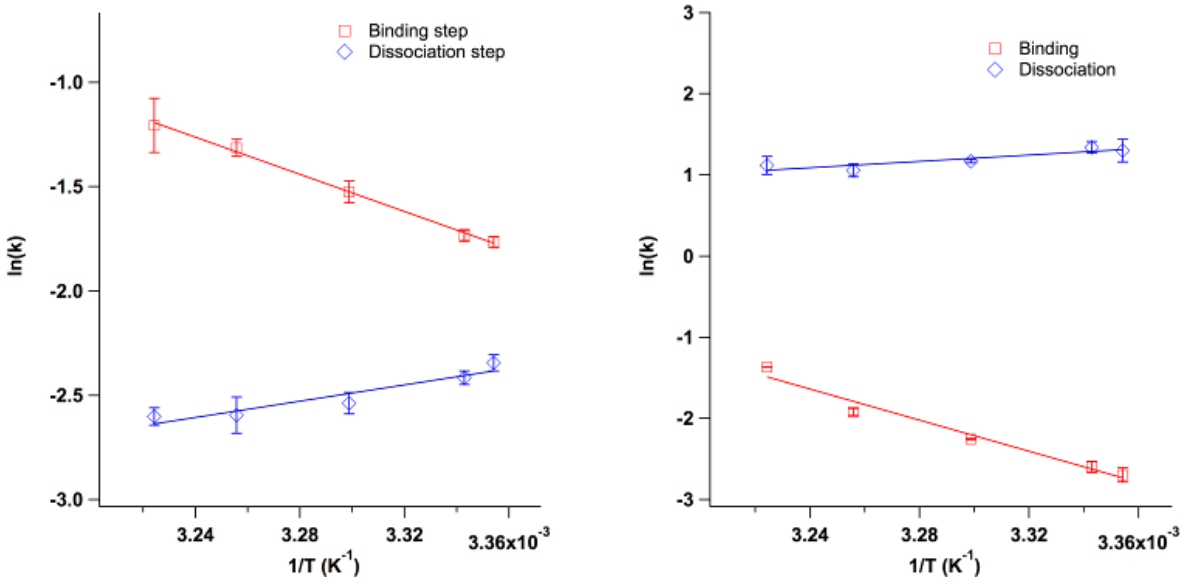

Figure 21. Arrhenius plot. (a) wild type (left) (b) methylated type (right). Single-molecule experiments were tested in 25, 26, 30, 34, 37 °C.

Left is the Arrhenius plot of the wild type (with no methylation) and right is that of methylated type. The activation energy of binding step is 8.874 kcal/K·mol with wild type, and 19 kcal/K·mol in the mythalylated type which can be inferred that thermodynamically it is more difficult to have a enzyme-DNA complex when the nucleic acid is methylated in the middle of the binding site. The gibbs free energy diagram based on the activation energy value can be drawn as figure 22 (C).

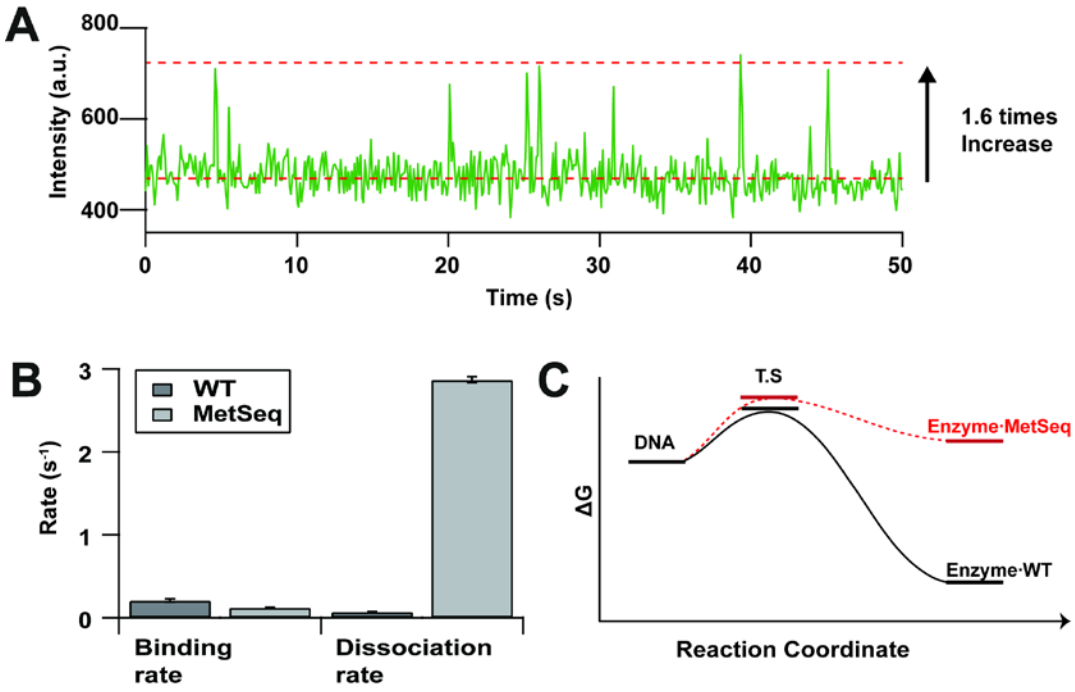

Figure 22. (A) A representative single-molecule fluorescence trajectory. With MetSeq, the 1.6-fold enhancement factor remained, but the duration time of enzyme bound state is dramatically shortening. (B) The comparison of reaction rate between WT and MetSeq. Note that the binding rate on MetSeq is slower than the binding rate on WT, implying the higher activation energy in enzyme binding reaction on MetSeq. (C) Expected free-energy diagram for WT (black curve) and MetSeq (red dashed curve) interacting with enzyme.

4.2.4. Simulation fitted with single-molecule data

The simulation was run with the chemical reaction rate constants obtained from the single-molecule experiments as below.

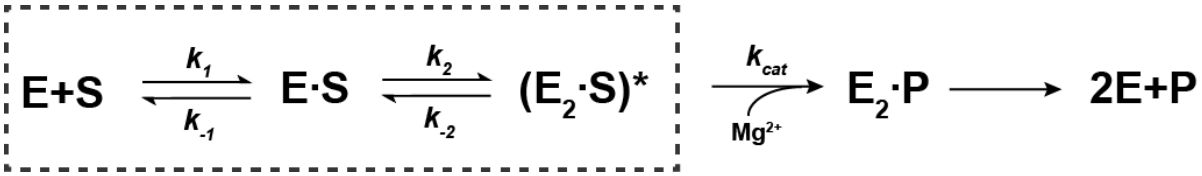

Concentration of E: [E], Initial concentration of E: $[E]_0$, Concentration of S: [S], Initial concentration of S: $[S]_0$ Concentration of ES: [ES], Concentration of ES*: [ES]*, Concentration of product: [P]

$$[E] = [E]_0-[ES]-[ES]^*$$

$$\frac{d}{dt}[S] = -k_1\cdot[S]([E]_0-[ES]-[ES]^*)+k_{-1}\cdot[ES]$$

$$\frac{d}{dt}[ES] = -k_{-1}\cdot[ES]-k_2\cdot[ES]+k_1\cdot[S]([E]_0-[ES]-[ES]^*)+k_{-2}\cdot[ES]^*$$

At equilibrim, $\frac{d}{dt}[ES] = 0$, $\frac{[ES]^*}{[ES]} = \frac{k_2}{k_{-2}} \equiv K_2$

Thus, $\frac{d}{dt}[ES] = -k_{-1}\cdot[ES]-k_2\cdot[ES]+k_1\cdot[S]([E]_0-[ES]-[ES]^*)+k_{-2}\cdot[ES]^* = 0$

$$\rightarrow \frac{d}{dt}[ES] = -k_{-1}\cdot[ES]+k_1\cdot[S]([E]_0-(1+K_2\cdot[ES]) = 0$$

$$[ES] = \frac{k_1\cdot[S][E]_0}{k_{-1}+k_1\cdot[S]+k_1\cdot K_2[S]}$$

$$[ES] = \frac{K_1[S]}{1+K_1[S]}[E0]$$

$k_{cat} \cdot K2 \cdot [ES] \propto d[P]/dt$

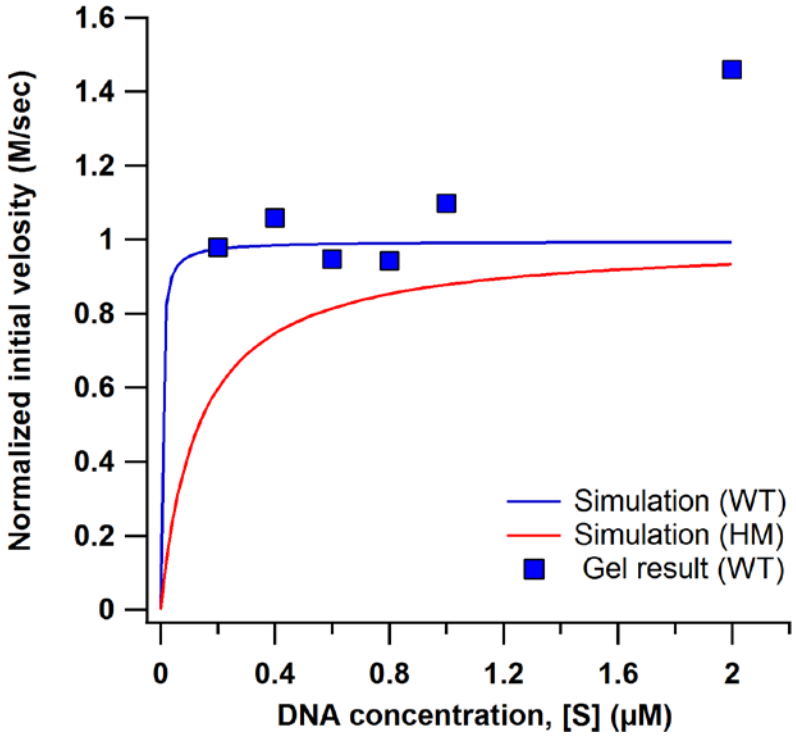

Figure 23 Simulation fitted with single–molecule data. The blue line is a simulation value of a wild-type, and the red line is a simulation value of a hemi-methylated type. The blue points were obtained from the single-molecule tests.

Interestingly, the ensemble agarose gel result was is in accord with the simulation result that was calculated with the single-molecule experiment data. More ensemble experiments are in need to prove the simulation and the assumptions that are counted in.

4.3 Conclusions

DNA methylation does not affect the rate of the binding, but the rate of the dissociation of the enzyme due to its thermodynamically unstability. The ensemble measurement and the single-molecule experiments data converge to the result that helps to understand the kinetics of unmethylated and methylated DNA-enzyme reaction.

5. Reference

1. Axelrod, D., Total internal reflection fluorescence microscopy in cell biology. *Traffic* **2001,** *2* (11), 764-774.
2. Axelrod, D., Cell-substrate contacts illuminated by total internal reflection fluorescence. *The Journal of cell biology* **1981,** *89* (1), 141-145.
3. Hwang, H.; Kim, H.; Myong, S., Protein induced fluorescence enhancement as a single molecule assay with short distance sensitivity. *Proceedings of the National Academy of Sciences* **2011,** *108* (18), 7414-7418.
4. Tomko, E. J.; Fischer, C. J.; Lohman, T. M., Ensemble methods for monitoring enzyme translocation along single stranded nucleic acids. *Methods* **2010,** *51* (3), 269-276.
5. Ha, T., Single-molecule fluorescence methods for the study of nucleic acids. *Current opinion in structural biology* **2001,** *11* (3), 287-292.
6. Pingoud, A.; Fuxreiter, M.; Pingoud, V.; Wende, W., Type II restriction endonucleases: structure and mechanism. *Cellular and molecular life sciences* **2005,** *62* (6), 685-707.
7. Watanabe, N.; Takasaki, Y.; Sato, C.; Ando, S.; Tanaka, I., Structures of restriction endonuclease HindIII in complex with its cognate DNA and divalent cations. *Acta Crystallographica Section D: Biological Crystallography* **2009,** *65* (12), 1326-1333.
8. Nwankwo, D. O.; Moran, L. S.; Slatko, B. E.; Waite-Rees, P. A.; Dorner, L. F.; Benner, J. S.; Wilson, G. G., Cloning, analysis and expression of the *Hin*dIII RM-encoding genes. *Gene* **1994,** *150* (1), 75-80.
9. Pingoud, A.; Jeltsch, A., Structure and function of type II restriction endonucleases. *Nucleic Acids Research* **2001,** *29* (18), 3705-3727.
10. Singal, R.; Ginder, G. D., DNA methylation. *Blood* **1999,** *93* (12), 4059-4070.
11. Tang, D.; Ando, S.; Takasaki, Y.; Tadano, J., Mutational analyses of restriction endonuclease—HindIII mutant E86K with higher activity and altered specificity. *Protein engineering* **2000,** *13* (4), 283-289.
12. Selvin, P. R.; Ha, T., *Single-molecule techniques: a laboratory manual*. Cold Spring Harbor Laboratory Press Cold Spring Harbor, NY: 2008.
13. Berg, J. M.; Tymoczko, J. L.; Stryer, L., *Biochemistry, International Edition*. WH Freeman & Co. New York: 2006.
14. Winkler, F. K.; Banner, D. W.; Oefner, C.; Tsernoglou, D.; Brown, R.; Heathman, S.; Bryan, R.; Martin, P.; Petratos, K.; Wilson, K., The crystal structure of EcoRV endonuclease and of its complexes with cognate and non-cognate DNA fragments. *The EMBO Journal* **1993,** *12* (5), 1781.
15. Jeltsch, A., Beyond Watson and Crick: DNA methylation and molecular enzymology of DNA methyltransferases. *Chembiochem* **2002,** *3* (4), 274-293.
16. Reik, W., Stability and flexibility of epigenetic gene regulation in mammalian development. *Nature* **2007,** *447* (7143), 425-432.
17. Shi, X.; Lim, J.; Ha, T., Acidification of the oxygen scavenging system in single-molecule fluorescence studies: in situ sensing with a ratiometric dual-emission probe. *Analytical chemistry* **2010,** *82* (14), 6132-6138.

Appendix

6. Optimal Condition for enzyme activity

6.1 Ion concentration

To find the most optimal condition for the enzyme activity, concentrations of $MgCl_2$ and NaCl were controlled. Enzyme activity highly depends on the Mg^{2+} ion concentration (Figure 24). Enzyme activity of catalytic was most activated when Mg^{2+} was 50 nM. NaCl was also tested and verified that sodium ion concentration does not affect the enzyme activity. To test the effect of monocation, KCl was substituted for NaCl. KCl concentration also did not show dependence on enzyme activity (Figure 25). The first column of figure 25 represents the best combination of the ion concentration for the enzyme activity. As it demonstrates, the enzyme activity which is correlated with the fraction ratio is the highest with 50 nM of Mg^{2+}, whereas sodium, or potassium ion has no effects on the activity.

6.2 Reaction in imaging buffer

In ensemble test, the enzyme activity was most activated in the buffer containing 50 mM Tris pH 8.0, 50 mM MgCl2, 50 mM NaCl, and water. In single-molecule test, the buffer condition is different because Trolox, glucose, pyranose oxidase, and catalase were used to visualize the fluorescent molecules. Molecular O_2 causes photobleaching which disturbs the observation of the kinetics of a fluorescent dye. Glucose and pyranose oxidase are the oxygen scavenging system that eliminates the oxygen.[17] Also with the oxygen scavenging system, Trolox is used to reduce photobleaching.[17] To examine the effect of the imaging buffer, enzyme was incubated in each buffer for 10 minutes at 37 °C. In figure 26, it confirms that IB does not affect the enzyme activity. The fraction ratio demonstrates the amount of dsDNA that was cleaved by *Hin*dIII. It was measured by ImageJ.

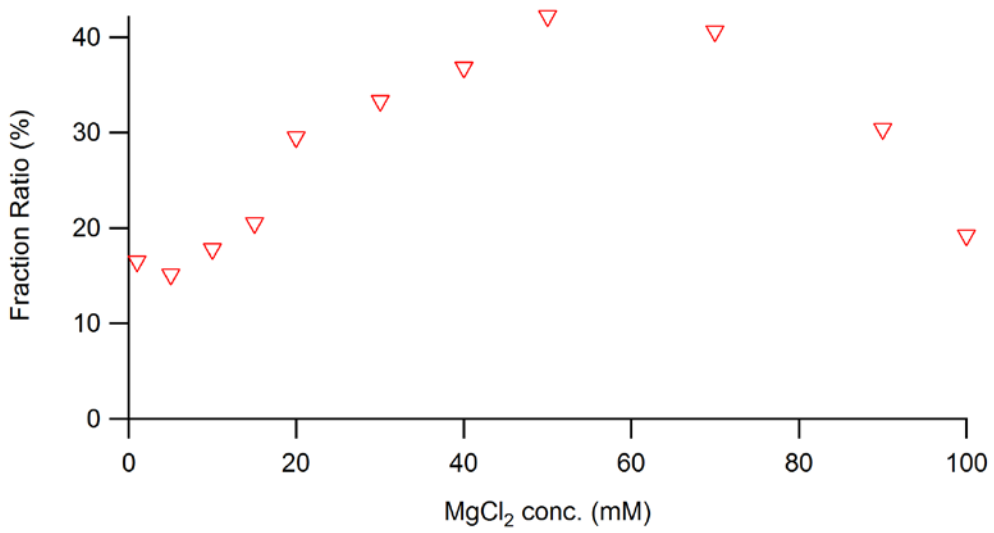

Figure 24. Mg^{2+} ion dependence on *Hind*III enzyme activity. The reaction was run in buffer with 50 mM of NaCl for 30 minutes at 37 °C.

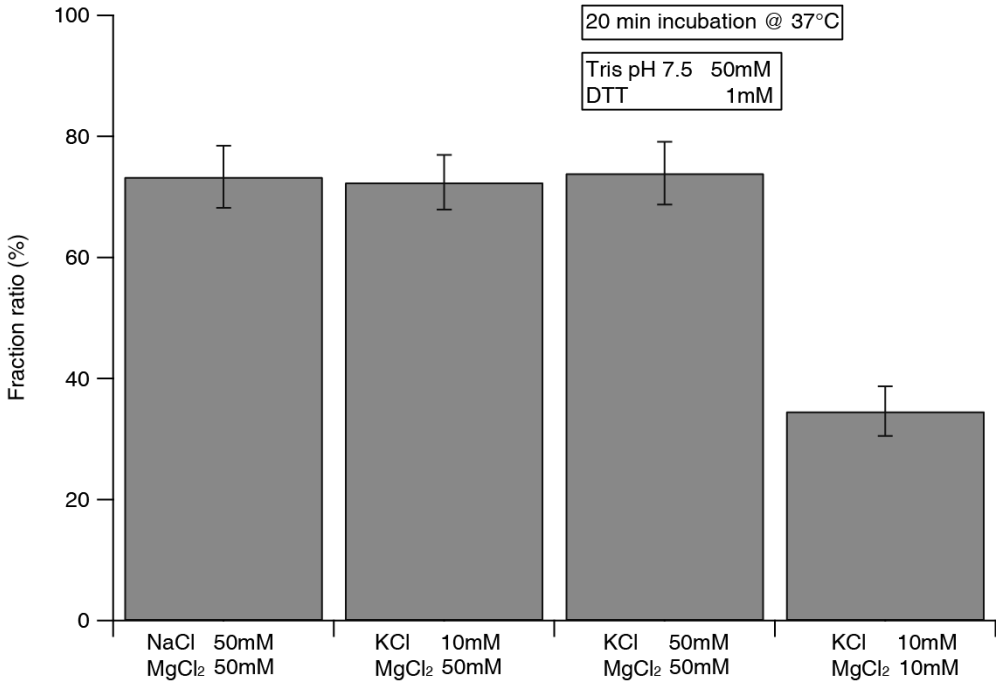

Figure 25. Ion dependence on enzyme activity. Various concentrations of NaCl, and KCl were tested for enzyme activity.

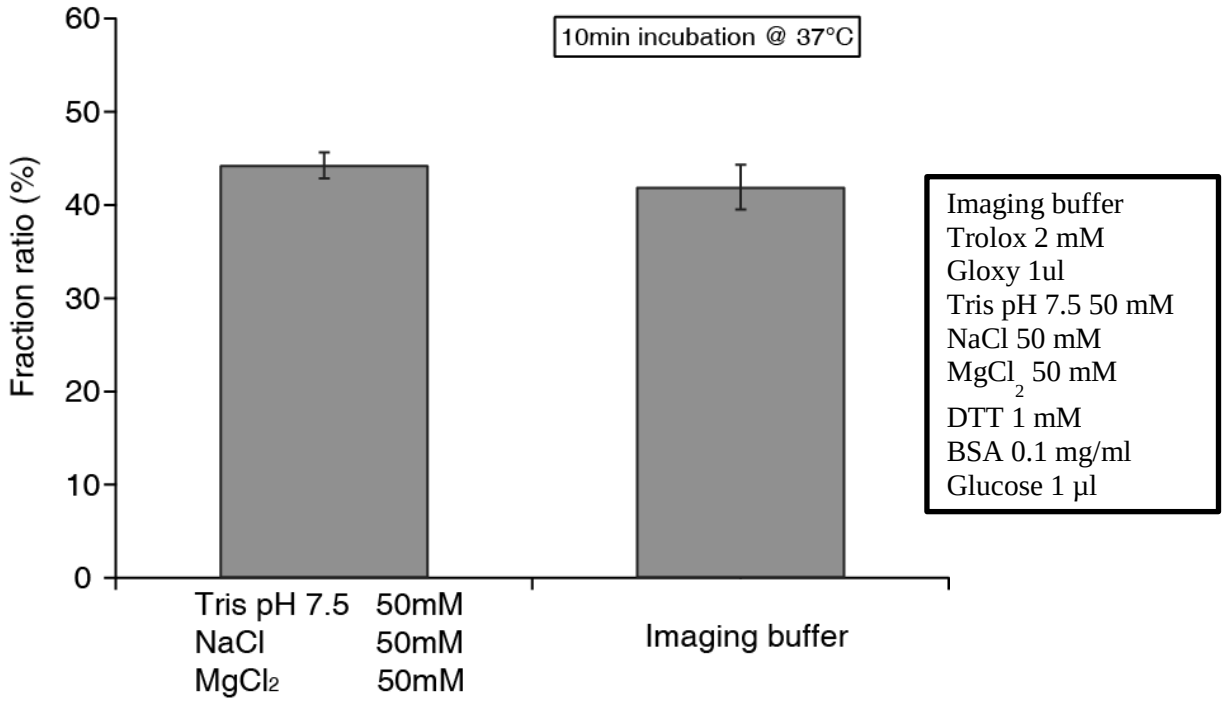

Figure 26. Enzyme activity test in imaging buffer. Imaging buffer including triplet quenchers is mandatory in single-molecule experiments.

6.3 Enzyme activity on wild type vs. fluorophore labeled dsDNA

Cy3 fluorophore is labeled at 3bp far from the recognition site of the enzyme (AAGCTT) which can block the enzyme binding or disturb the interaction of the dsDNA – protein. Prior to the TIRF single-molecule test, it was necessary to test the effect of Cy3 fluorophore labeling. In figure 27, a control sample was B which both ssDNA do not have any modifications. A is the sample with Cy3 labeled on one strand of the labeled substrate. Both samples (~2 μM) were incubated in a buffer with enzyme (~35 nM) at 37 ˚C for 20 minutes. The labeled substrate shows less than 10 % lower enzyme activity. The third lane is enzyme activity of the wild type substrate without Mg^{2+} ion in reaction buffer. The enzyme does not appear to have any endonuclease activity without Mg^{2+} ion.

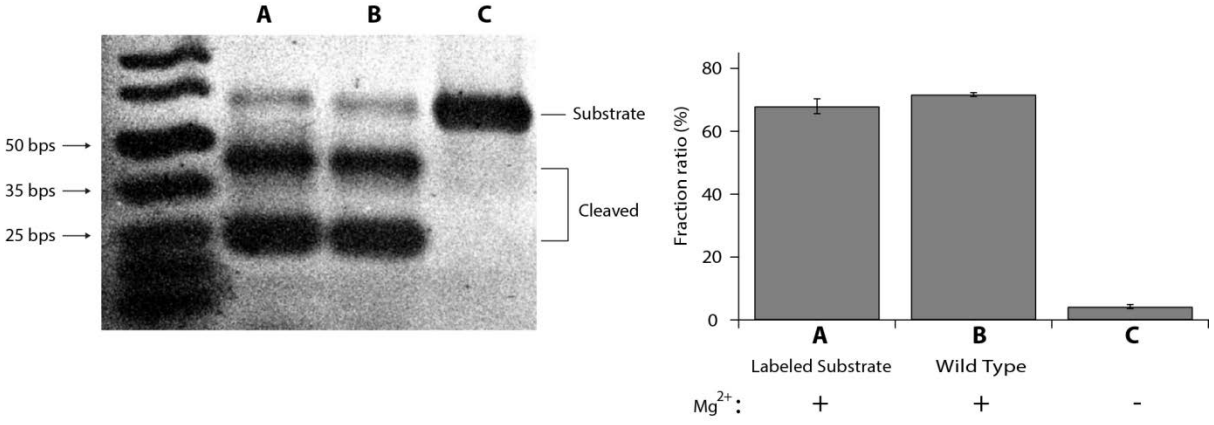

Figure 27. Effects of fluorophore labeled strand on *Hind*III enzyme activity. A lane represents the substrate which is labeled with Cy3 flurophore on 3bp far from the recognition site, B lane represents the wild type substrate with no modifications and C lane represents the wild type substrate in buffer without Mg^{2+} ion. A and B lane show three bands of cleaved fragments. Each fragment demonstrates 66 bp (full length), 25 bp and 41bp. C lane shows no activity of enzyme.

6.4 Time trajectory of a single molecule.

A time trajectory of a single Cy3-labeled substrate shows the fluctuations as the enzyme was injected to a reaction chamber. After about 70 seconds of constant fluctuations, the Cy3 fluorescent dye was quenched and shows no more signals. This trace provides several information about the DNA-enzyme interaction. First, enzyme injection indeed increases the intensity of fluorescence in a regular base. Second, the fluorescence intensity enhancement factor is constant. Third, the substrate and enzyme concentration was appropriate to avoid the overlapping of fluorophores.

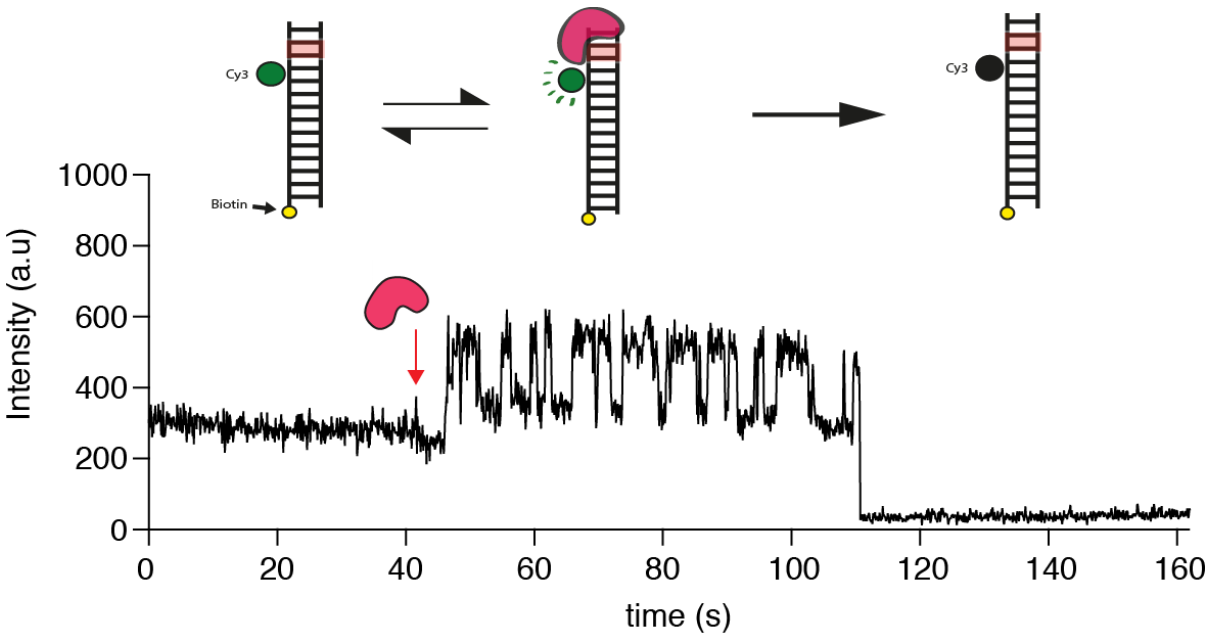

Figure 28. Time trajectory of a single molecule. *Hin*dIII was injected after 40 seconds, and the after the fluorescence fluctuations, the dye quenched at 110 seconds.

국문초록

DNA 매틸화는 진핵생물 세포와 원시핵 생물 세포 내에서 모두에서 중요한 역할을 하고 있습니다. 진핵 생물에서는, gene regulation 을 조절하기도 하고, 원시핵 생물 특히 박테리아에서는, 외부로부터 침입하는 유전자로부터 자신을 지키는 역할을 하기도 합니다. 지금껏, DNA 매틸화에 대해 많은 연구가 되어 오고 있지만, 대부분이 ensemble 수준에서 연구된 것입니다. 이번 연구에서 우리는 DNA 매틸화가 DNA 와 단백질관의 상호관계에 주는 영향에 대해 단분자 수준에서 연구하고자 합니다. 단백질이 DNA 에 붙고 떨어지는 속도를 구하여서, DNA 가 매틸화 되어있을 때 붙고 떨어지는 속도를 비교하였습니다. 또한, 단분자 수준에서 구한 동역학적 값들이 ensemble 수준에서 값으로 수렴하는 것을 볼 수 있었습니다. 더 나아가, DNA 가 매틸화 되어있을 때는 동역학 매커니즘의 특정 부분이 영향을 받는 것으로 밝혀졌습니다.

주요어: 단분자 테크닉, 전반사 형광 현미경, 제한 효소, *Hind*III, DNA−단백질 상호작용, DNA 매틸화

학번: 2011−23221

이학석사학위논문

Single-molecule Fluorescence Study for the Effects of DNA Methylation on the Association and Dissociation Kinetics of Restriction Endonuclease and DNA

DNA 메틸화가 제한효소와 DNA 결합 및 분해
동역학에 주는 영향에 대한 단분자 형광 연구

2014년 2월

서울대학교 대학원

화학부 물리화학전공

박 소 영

MS. Dissertation

Single-molecule Fluorescence Study for the Effects of DNA Methylation on the Association and Dissociation Kinetics of Restriction Endonuclease and DNA

February 2014

Research Advisor:

Professor Seong Keun Kim

Department of Chemistry

Seoul National University

So Young Bak

Abstract

Single-molecule fluorescence study for the effects of DNA methylation on the association and dissociation kinetics of restriction endonuclease and DNA

So Young Bak

Department of Chemistry

The Graduate School

Seoul National University

DNA methylation plays a great role both in eukaryotic and prokaryotic cells. In eukaryotes, it suppresses gene regulation, whereas in prokaryotes, specifically in bacteria, it protects the cell from invasion of foreign genes. Many studies have been carried out for the effect of DNA methylation at the ensemble level, but in this study, we investigated the effect of DNA methylation on DNA-protein interaction by single-molecule fluorescence to understand the interaction at the molecular level. We measured the association and dissociation rates of native as well as methylated DNA and found that the values converge to the corresponding ensemble rates. We were able to differentiate the kinetics of association, and dissociation and found that our result was consistent with the fact that DNA methylation interrupts the DNA- protein interaction, especially at a specific kinetic

step.

Keywords: Single-molecule technique, Total internal reflection fluorescence microscopy, Restriction endonuclease, *Hin*dIII, Protein-DNA interaction, DNA methylation

Student Number: 2011-23221

Table of Contents

1. Introduction

Observation and detection of kinetics and dynamics of biomolecules have drawn attention to many scientists because understanding the phenomena of the biomolecules are intimately related to humans. These are mostly studied in bulk materials, in which the kinetics of the hundreds and thousands of biomolecules are averaged out in ensemble and show the trend of a majority in a condition. The desire to scope down to an individual molecule and observe the kinetics of one molecule has developed the single-molecule technique. The single-molecule technique allows us to solve our curiosity of observing the hidden steps of protein kinetics that otherwise are indistinguishable at the ensemble level.[1] While ensemble tests provide an averaged value, a single-molecule technique distinguishes one molecule at a time and gives information of kinetics and conformational changes of proteins and DNA.

Single-molecule tools are put in a category by various standards. Total internal reflection fluorescence microscopy, TIRF, is categorized as an immobilization-based technique that is one of the most popular single-molecule techniques that draws a trajectory of a single molecule while it is immobilized on a surface of a quartz. The immobilized molecules are generally labeled with a fluorescence dye, and the fluorescence dye molecules are visualized when the dye molecules are excited by evanescent wave that is generated at the interface of the quartz and the aqueous solution.

In this study, we used TIRF to observe the kinetics of restriction endonuclease, *Hin*dIII. The experiment was designed to employ the photophysical property of Cy3 rather than FRET which is another popular way of detecting kinetics of proteins. Through analysis of the observed association and dissociation, the effects of methylation can be elucidated.

2. Basic Principles

2.1 Total internal reflection fluorescence microscopy

Optical configurations

Total Internal Reflection Fluorescence, TIRF, is a type of fluorescence assay that detects the kinetics of a single molecule at a low concentration. We used a diode laser (532nm) with 100mW (TECGL-30, World Star Tech.). The light passes through the Pellin Broca Prisms (PLBC-5.0-79.5-SS) and the fluorescence of the samples are excited by evanescent field generated by total internal reflection. The fluorescence enters the EMCCD (Andor; DU-897E-CS0-#BV) with exposure time of 100 ms and visualized by IDL software. The visualized molecules are analyzed with MATLAB program. Through selective excitation of the immobilized fluorophores, TIRF enables to track a single molecule for a range of time with high signal-to-noise ratio. Figure 1 is the scheme of the setup.

Total internal reflection fluorescence

When light travels from a higher refraction index medium to a lower refraction index medium, the light changes its pathway according to Snell's law. If the incident angle is greater than the critical angle, the light does not pass through the medium, but totally reflects. Total internal reflection induces an electromagnetic field of evanescent field which decays exponentially from an interface of a quartz. The penetration depth of TIRF is shallow (~150 nm) and excites the fluorophores which are immobilized in the range of ~150 nm from the surface of the quartz. The characteristic of exponential decay of evanescence field avoids the background noise from the fluorophores which are not immobilized, and improves the signal-to-noise ratio critically.

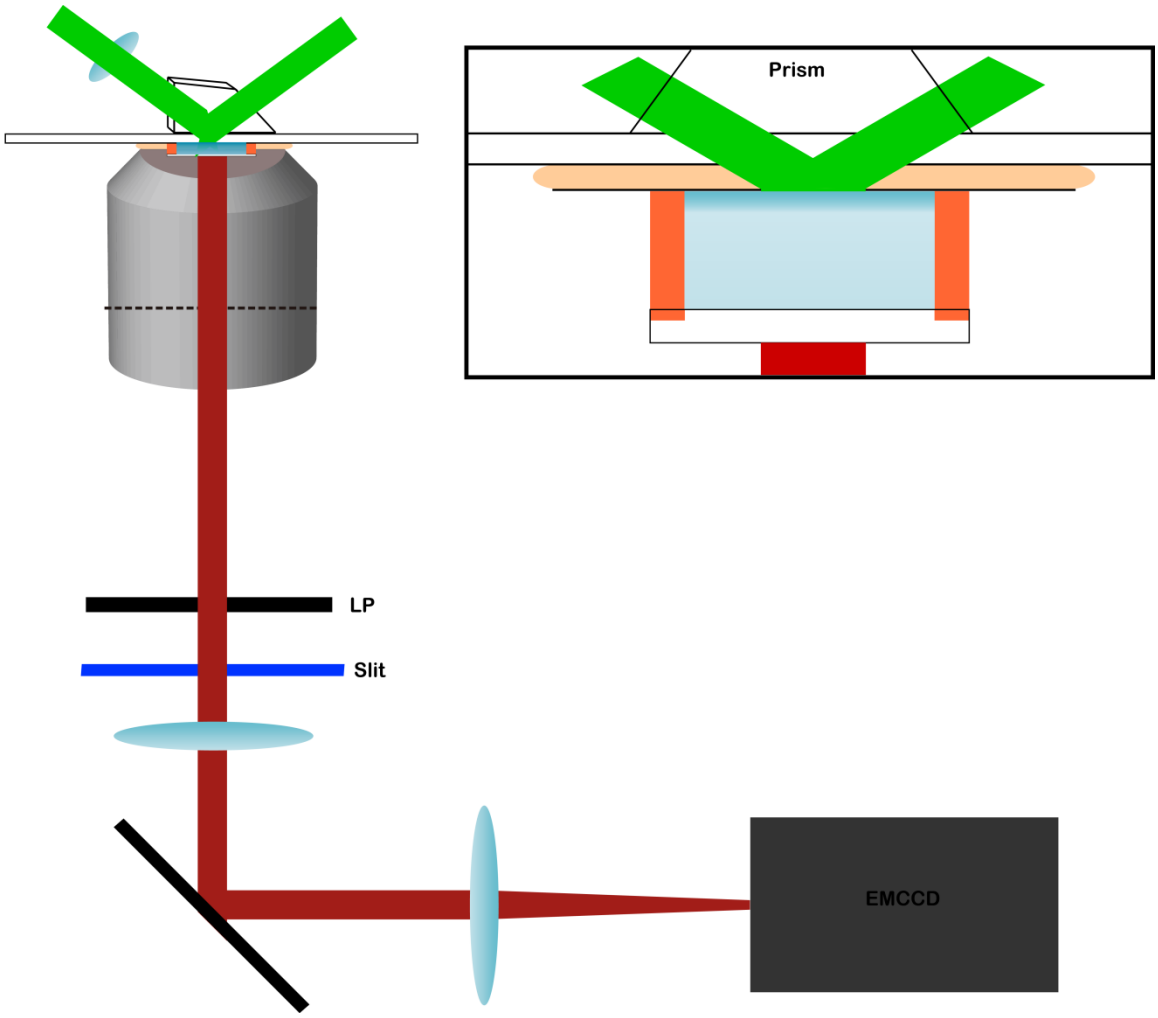

Figure 1. Scheme of the TIRF setup. Green ray indicates the laser source (532 nm), the blue area indicates the evanescent field generated from total internal reflection, and the LP stands for long pass filter.

Prism-based TIR.

Prism is used to generate the total internal reflection and evanescent field. The refractive index of prism is about 1.45 which is close to that of quartz. The immersion oil with refractive index 1.45 is used to eliminate any refractive index difference. The incident light passes through a prism, quartz and then on the surface of aqueous buffer with refractive index 1.33, it deflects according to Snell's law. Snell's law is applied as below:

$$n_1 \sin \Theta_1 = n_2 \sin \Theta_2$$

$$\sin \Theta_1 = \frac{n2}{n1} = \frac{1.33}{1.45}$$

$$\Theta_1 = 66.5^{\circ}$$

Θ_2 is 90 degrees at a critical angle. When incident angle is steeper than the critical angle, 66.5˚, the light totally reflects, and generates the evanescent field.

Evanescent field is an electromagnetic field that penetrates into the liquid medium between a quartz and coverslip. *I* is an intensity and *z* is the perpendicular distance from the surface of a quartz.

$$I = I_0 \exp(-\frac{z}{d})$$

$$\mathrm{d} = \frac{\lambda}{4\pi n_2}\left(\frac{sin^2\,\theta}{sin^2\,\theta c} - 1\right)^{-1/2}$$

d is the exponential decay depth, θ_c is the critical angle of incidence, θ is the angle of incidence light, λ is the wavelength of incident light in vacuum, and n_2 is the refractive index of the aqueous medium in our case. θ should be greater than θ_c. This equation drives that the depth of evanescent field increases with decreasing θ. The depth of the evanescent field can be controlled by the angle of incidence light.[2]

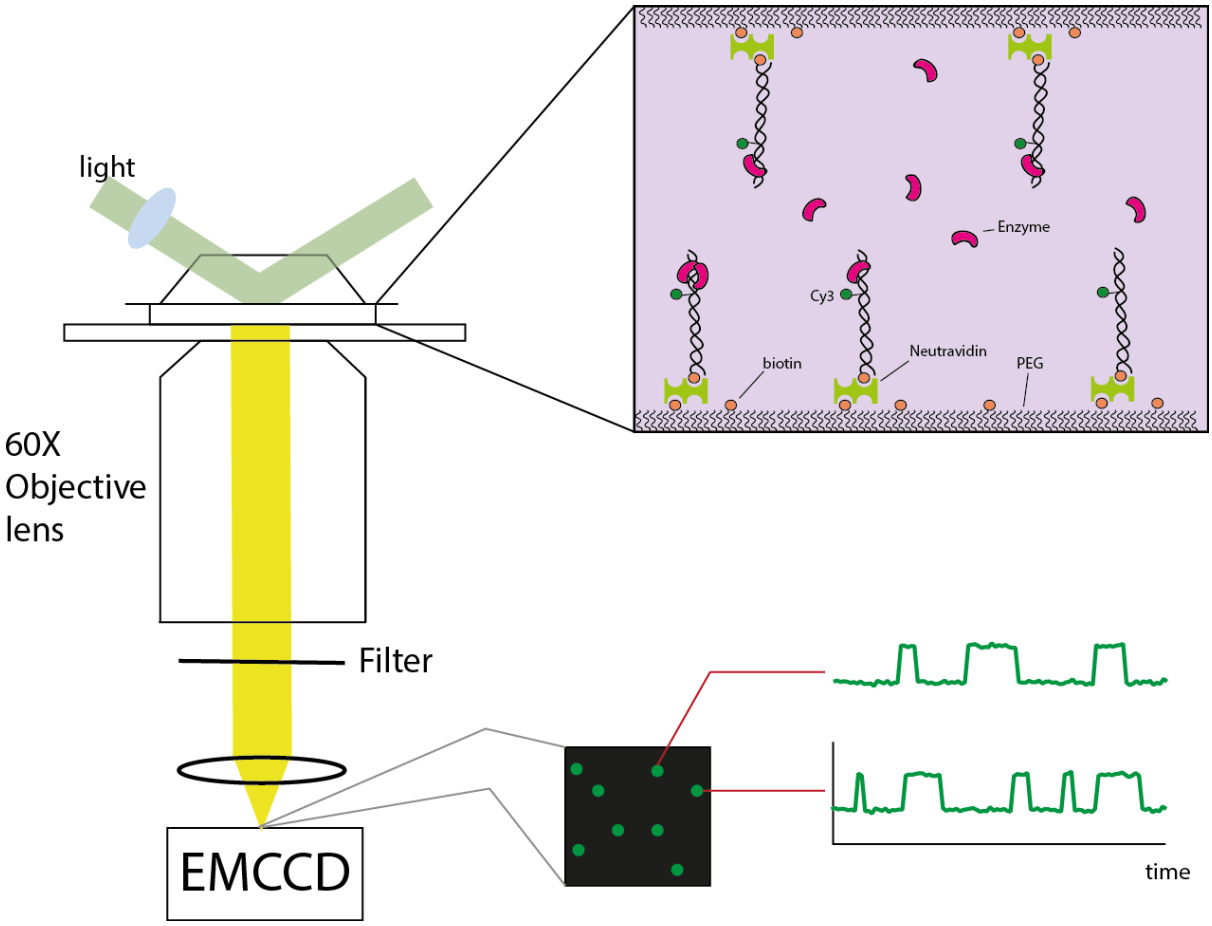

Figure 2. Prism type TIR: incident light with greater than the critical angle creates total internal reflection, and induces evanescent field. The molecules immobilized on the surface of a quartz are excited by evanescent field. Individual molecules can be tracked.

2.2 Protein binding induced fluorescence

Helen Hwang et al. addressed that the fluorescence dyes which bear *cis-trans* isomerization have protein binding induced fluorescence, PIFE, effect.[3] Fluorescence of *cis-trans* isomerizable dyes including Cy3 and Cy5 are enhanced by protein binding nearby and this property has been used in stopped-flow.[4] The mechanism of PIFE is not elucidated yet, but it is often used to observe the kinetics of a molecule. In this study, Cy3 was labeled 3bp far from the *Hin*dIII recognition site. The PIFE effect stated by Hwang was examined with the fluorophore labeled on the base of the oligonucleotides. Similar PIFE effect was observed with the fluorescence dye labeled on the backbone of DNA oligonucleotides. The PIFE effect that is address in this study is all based on the interaction between the protein and DNA with Cy3 labeled on a backbone. Protein association on dsDNA with Cy3 labeled nearby induces the fluorescence enhancement and dissociation decreases the fluorescence.

Fluorescence Resonance Energy Transfer, FRET, is a convenient technique to study the dynamics and kinetics of molecules. However, labeling fluorophores on a protein or DNA is inefficient and time consuming. Also, FRET is limited to its pair that energy can be transferred from a donor to an acceptor. FRET is useful when the conformational change or dynamics occur between 3-8 nm.[5] On the other hand, employing the photophysical property of an isomerizable fluorophore such as Cy3 to study the kinetics of molecules has great advance in easy preparation. A complicated protein labeling and FRET pair are not required. For certain enzymes, fluorescence intensity library exists with base pair sensitivity.[3]

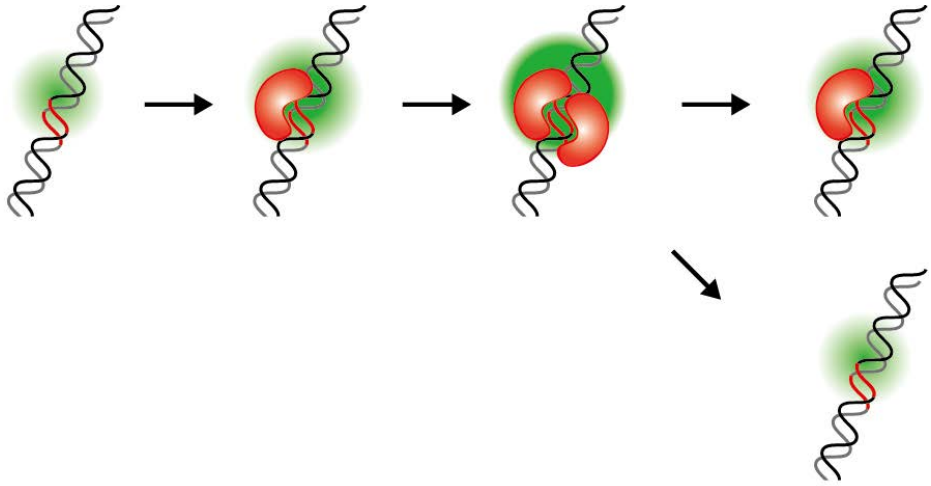

Figure 3. Scheme of protein induced fluorescence enhancement. The green area indicates the Cy3 labeling, and the red lines on the DNA indicates the specific site that the enzyme binds.

2.3 Restriction endonuclease, *Hin*dIII

*Hin*dIII is a type II restriction endonuclease which recognizes 4-8 specific sequence and cleaves the binding site with a cofactor Mg^{2+} ion.[6] *Hin*dIII recognizes and cleaves the palindromic sequence 5'-A/AGCTT-3'.[7] *Hin*dIII is comprised of 300 amino acids and has a molecular weight of 34.950 kDa.[8]

*Hin*dIII is a homodimer which activates its nuclease activity when two proteins compose a dimer along with the DNA. Figure 4 shows the crystal structure of *Hin*dIII endonuclease. Each red and blue chain is a single *Hin*dIII protein. They bind to the recognition site and cleave the site. The fundamental reaction mechanism of restriction endonucleases is known as hydrolysis of the phosphodiester backbone of DNA.[6, 9]

There were several standards to be satisfied for studying the effects of methylation to DNA and protein interactions. First, commercial enzyme must be available. Second, binding sequence should be well known. Third, the size should not be too big because its interaction with DNA can be disturbed by the fluorophore and difficult to observe the kinetics by TIRF. At last, the recognition sequence should have at least one cytosine for methylation because in prokaryotic and eukaryotic genes,

methylation occurs mostly at cytosine.[10] *Hin*dIII was appropriate for study of effects of methylation with the identified binding site and cytosine of the site (AAGCTT) that can be methylated. *Hin*dIII with 100,000 U/ml was purchased by New England Biolabs.

Mg^{2+} is a cofactor that binds between the DNA and protein and promotes the hydrolysis of the phosphodiester bond by water and cleaves the recognition site of *Hin*d III. Mg^{2+} ion can be replaced by other metal ions such as Mn^{2+} and Ca^{2+}. Several other divalent ions were tested for cleavage activity and the result that Ca^{2+} has the less cleavage activity coincide with the previous report by D.Tang.[11]

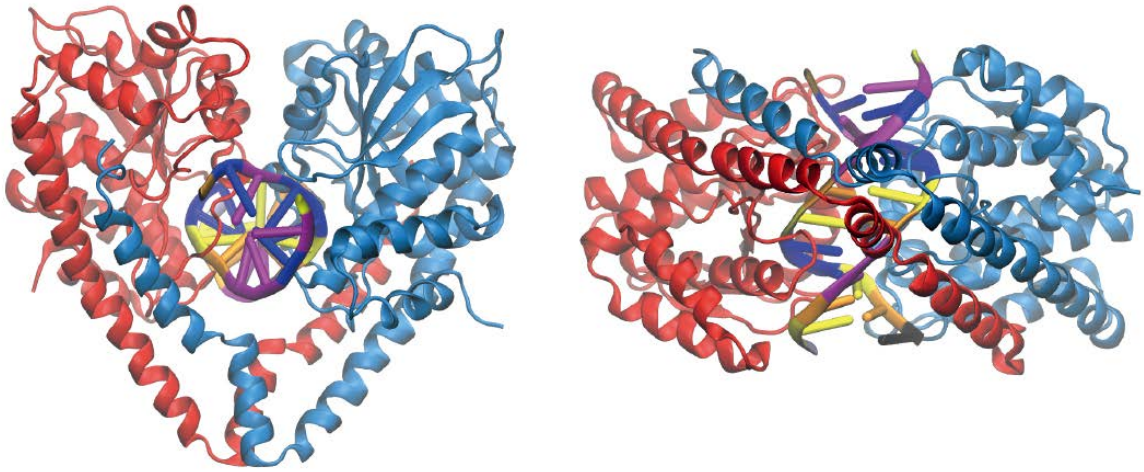

Figure 4. Structure of *Hin*d III. (Left) upper view, and (right) side view

2.4 Sample Preparation

DNA oligonucleotides

The following oligonucleotides (shown 5'-3') were used (manufactured by IDT DNA): GAATGCACGCATGCATCGATAAGCTTCGATCGATAGAAAAAAAAAAAAAAAAAAAAAA AAAAAAA (wild type complement strand), Biotin- TTTTTTTTTTTTTTTTTTTTTTTTTTTTT, TATTCGAAGC/iCy3/TAGCTATC (Cy3 labeled strand), GAATGCACGCATGCATCGATAAG/iMe-dC/TTCGATCGATAGAAAAAAAAAAAAAAAAAAAAAAAAAAAAA (Methylated complement strand), GAATGCACGCATGCATCGATAAATTTCGATCGATAGAAAAAAAAAAA AAAAAAAAAAAAAAAAAAA (NonSpecific complement). The oligonucleotides were PAGE purified when longer than 60 base pair, otherwise they were HPLC purified.

Quartz modification

The quartz (Prism Research Glass, Inc) were coated with polyethylene glycol, PEG, following the protocol from "**Single-molecule Techniques:** A Laboratory Manual" by Paul R. Selvin and Taekjip Ha. On the surface of an aminoxylane modified quartz, m-PEG (Laysan Bio) and biotin-PEG (Laysan Bio) are spread with 80:1 ratio. 0.1 mg/ml neutravidin is added on the surface of a quartz and incubated for 10 minutes.[12] Neutravidin is applied on a surface to immobilize the biotylated DNA substrates. The substrate is biotylated at 5' end, and Cy3 dye labeled in the middle with NHS ester link. About 20 pM of the substrates are applied on top of the surface, and incubated for 10 minutes. DNA substrates are immobilized on the quartz through neutravidin-biotin interaction. The surface of a quartz is then washed with T50 buffer (10mM Tris-HCl pH 8, 50 mM NaCl). Imaging Buffer, IB, is required to visualize the fluorophores. IB contains Tris pH 8 (0.1 M), Trolox ((±)-6-Hydroxy-2,5,7,8-tetra-methylchromane-2-carboxylic acid; Fuka)[12], NaCl, DTT, Bovine serum albumin (BSA; New England Biolabs), T50, glucose, and Pyranose oxidase from Coriolus sp.(Sigma-Aldrich).

The fluorophore labeled substrates are immobilized on a surface of a quartz through biotin-neutravidin interaction. Right after IB is applied on a surface with the substrates, place the quartz on an objective lens and view the molecules.

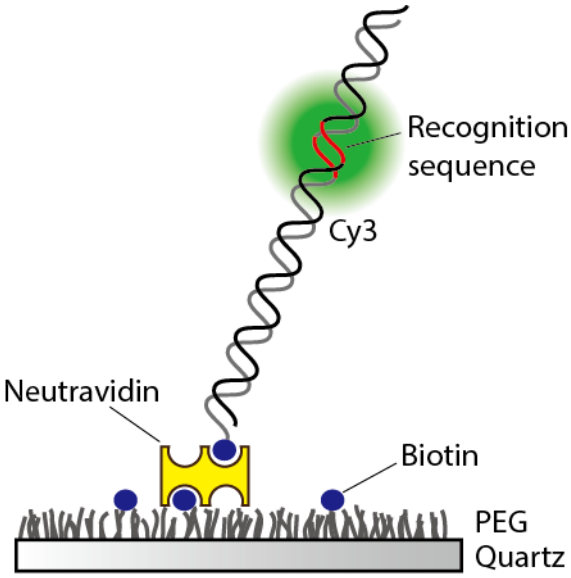

Figure 5. Immobilized dsDNA substrate on a PEG-coated quartz through biotin-neutravidin interaction. Recognition sequence is indicated in red, and the Cy3 fluorophore as a green area over the sequence.

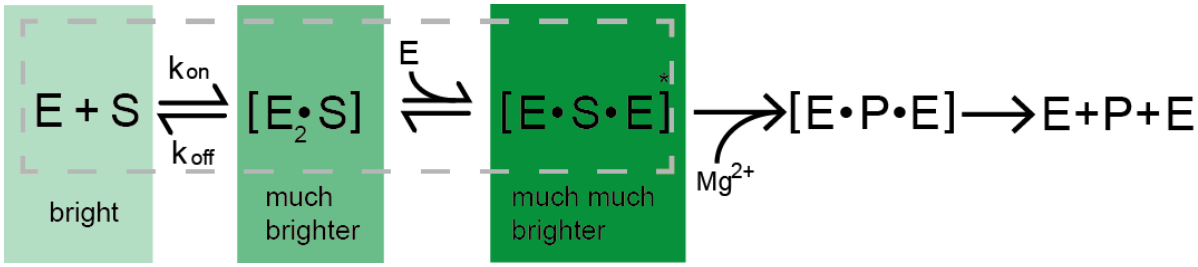

Figure 6. Expected reaction flow scheme.

3. A Novel way of detecting the protein association and dissociation dynamics and the dimer formation of a protein

3.1 Introduction

Understanding the dynamics of proteins comprises much information of protein-protein and protein-DNA interaction. Furthermore, understanding dynamics of a single protein can determine the hidden steps which were not observed in bulk material, and elucidate the interactions more accurately.

The association and dissociation dynamics of a restriction endonuclease *Hin*dIII was observed at a single-molecule level with TIRF. Each association and dissociation rate was determined. Transient state of conformational change followed by the association of the protein was observed with PIFE effect as well.

We report that kinetics of a protein can be studied with a fluorescence assay at a molecular level. Reaction rate such as association and dissociation rates were determined by the single molecule kinetics study.

*Hin*dIII is known as homodimer which requires two units of protein to have a catalytic activity. The reaction was expected as figure 6. E indicates *Hin*dIII restriction endonuclease, S as DNA substrate, and P as products which are cleaved. Enzymes associate with the DNA substrate that has specific binding sequence, and as enzyme binds to the substrate, the fluorescence of Cy3 is increased by PIFE effect. Enzyme and substrate complex itself is inefficient in enzyme activity, but when a *Hin*dIII dimer is formed, it is completely bound to the substrate and the conformational change which increases the fluorescence by tighter complex occurs.

3.2 Experimental

3.2.1 Fluorescence enhancement

The biotylated DNA substrate with *Hin*dIII binding sequence was first incubated with *Hin*dIII enzyme to confirm whether the fluorescence is enhanced when cis-trans isomerizable dye Cy3 is labeled in the vicinity of the protein binding sequence. Figure 7 shows wild type sequence and the distance between the Cy3 fluorophore and the recognition. As type II restriction endonuclease, the recognition site is in which the enzyme binds to. In order to find the optimal nucleic acid labeled to have the brightest intensity when a protein binds, we labeled Cy3 at different bases. From one base far from the recognition site (AAGCTT) to the tail of the DNA, Cy3 was labeled at various bases and tested for the optimal condition for PIFE effect. When Cy3 was labeled right next to the recognition site, the Cy3 signal was not enhanced with the enzyme, and it can be assumed that Cy3 fluorescent molecule disturbed the binding of a protein. On the opposite side, when Cy3 was labeled at the tail of the DNA, the PIFE effect could not be observed enough to analyze. The enhancement was subtle, and finally the optimal position was in which 3 bases far from the recognition site.

The figure 8 shows that the enzyme, *Hin*dIII, injection increased the fluorescence in ensemble. It was measured with a fluorometer in imaging buffer. The buffer with DNA substrates have an emission fluorescence of Cy3 at around 560 nm, and after the injection of enzyme in buffer, the intensity of the fluorescence increased. The green area indicates the increased amount of fluorescence. The phenomenon of fluorescence intensity increment through protein injection was also confirmed as protein binding at a single-molecule level by TIRF. In figure 9, the panel on the right side is a view of EMCCD. Each white spot indicates fluorophore of a molecule immobilized on a quartz surface. When the dsDNA with enzyme specific binding sequence are incubated with enzyme, the white spots became much brighter. The upper view without the enzyme contrasts from the one below. The view with the enzyme definitely shows brighter fluorescence. In figure 9, the single exponential graph of Gaussian function was changed to the bimodal distribution with the injection of the enzymes.

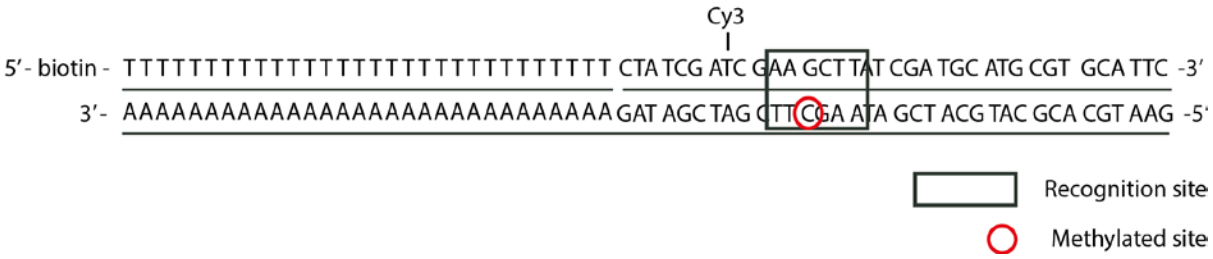

Figure 7. Sequence of dsDNA. The recognition site of *Hin*dIII is AAGCTT. Cy3 fluorescent is labeled three bases far from the sequence. For the methylated sequence, the cytosine in the middle of the recognition site opposite to Cy3.

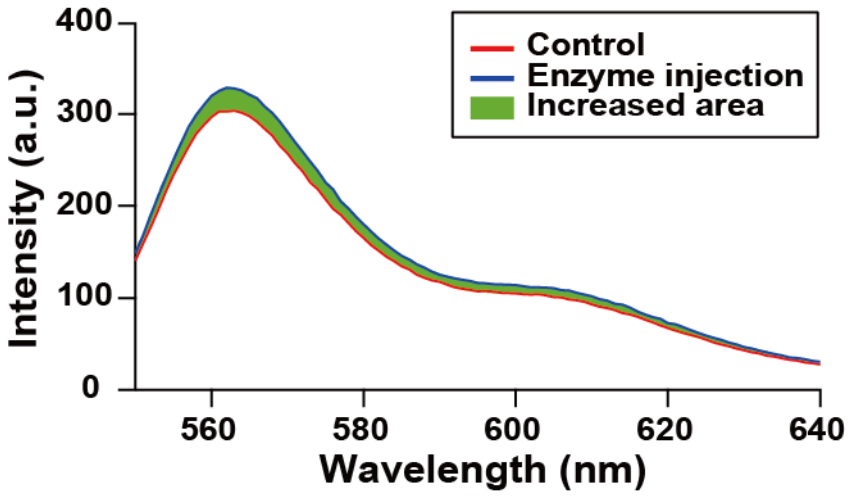

Figure 8. PIFE effect in ensemble. Increased fluorescence after enzyme (*Hin*dIII) injection was measured by fluorometer

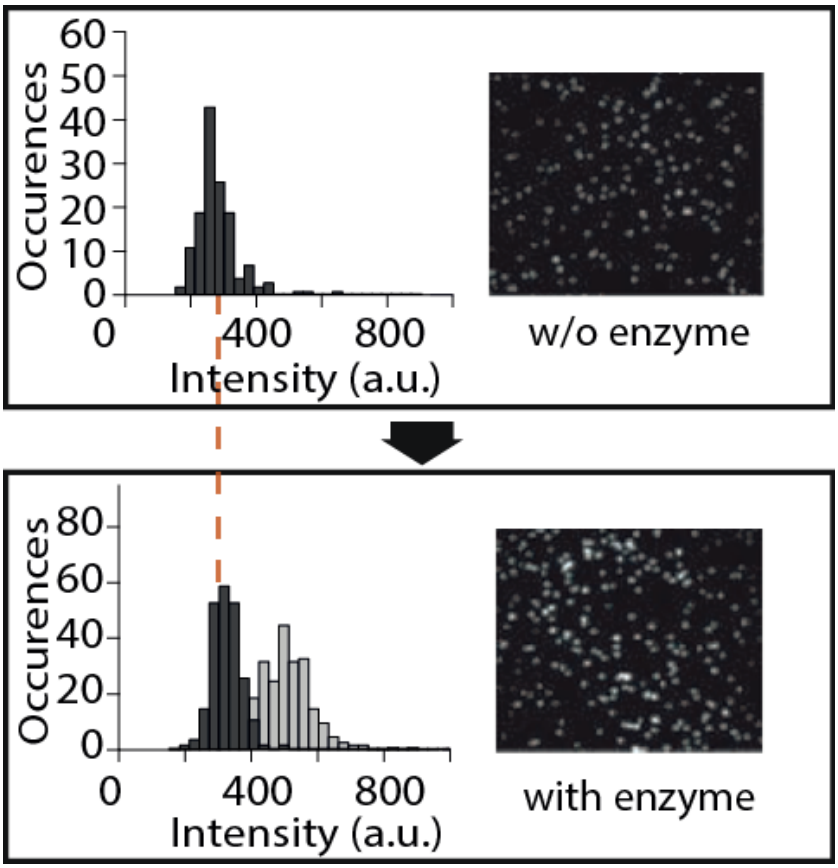

Figure 9. PIFE effect in single-molecule. (Upper) Wide-field images before the *Hin*dIII injection, and histograms of fluorescence intensities. (Below) After the enzyme injection, the fluorescence function was changed to the bimodal function.

3.2.2 Kinetic analysis of association and dissociation

The figure 10 is a scheme of DNA and protein interaction at TIRF. The DNA substrates are immobilized on a surface of a quartz by biotin-neutravidin interaction. The DNA substrates are labeled with Cy3 near the binding sequence of *Hin*dIII. While proteins are repeating the association and dissociation with the divalent ion, Ca^{2+}, k_{on} and $k_{off,}$ which indicate the rate of association and dissociation respectively, are calculated. Applying PIFE effect, TIR is utilized to give a fluorescence trajectory of a single molecule which increases the fluorescence as the protein binds near the Cy3 where recognition site exists.

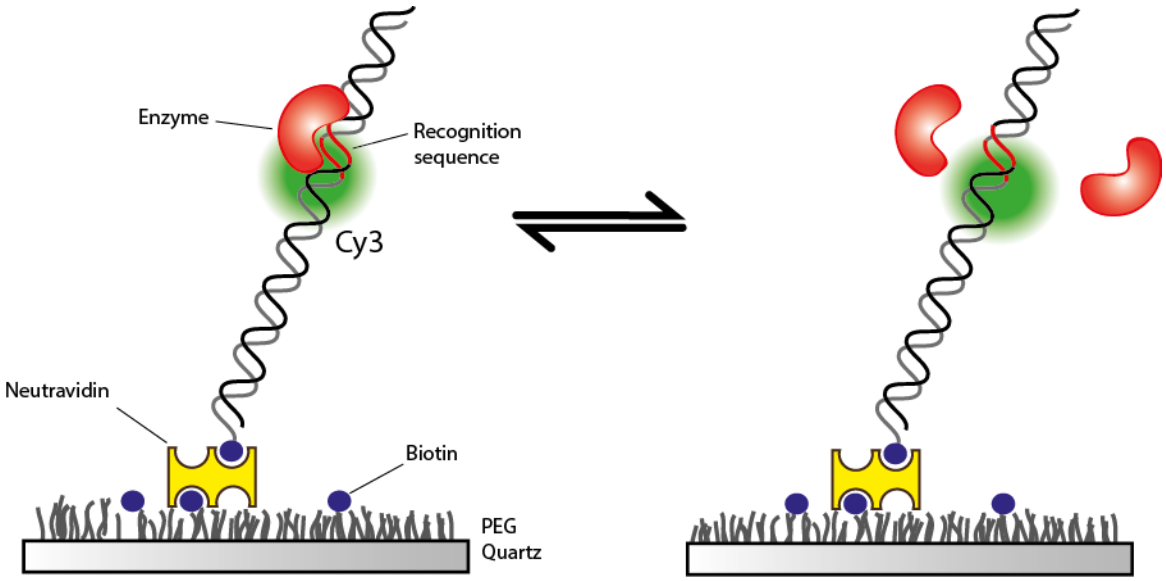

Figure 10. Single-molecule scheme of DNA and enzyme interaction on a substrate-immobilized quartz.

3.3 Results and Discussion

3.3.1 Reaction time in ensemble

Prior to the single-molecule test, the reaction time should be measured and confirmed that it is short enough to be observed at a single-molecule level. 2 μM dsDNA was incubated with the reaction buffer (buffer condition is indicated in figure11) for 1, 5, 10, 20, 30 and 40 minutes and the reaction was quenched by adding EDTA (0.4 M final). The fraction ratio is correlated to the enzyme activity, and shows how fast the reaction is. The catalytic rate, or also called the turn-over rate, K_{cat} of *Hin*dIII is 9.53 x 10^2/min.[11] In figure 11, after 20 minutes, over 80% of fractions were produce confirming that the reaction is fast enough to be tested at a single-molecule.

3.3.2 Enzyme concentration

Concentration of enzyme varied from 1 to 5 nM, while concentration of substrate dsDNA was about 1.2 μM. The fraction ratio was proportional to the concentration of enzyme, and showed the linear fit.

3.3.3 Specific vs. Nonspecific binding

We prepared dsDNA containing *Hin*dIII recognition sequence (AAGCTT, wild type, WT), and non-recognition sequence (AAATTT, NonSeq). Figure 18 (A) is a three different sets of sequence; Wild Type, Methylated sequence, and sequence without the recognition site. HPLC-purified sample was Cy3-labeled at 3 bps far away from the recognition site. Using agarose gel analysis, we tested the catalytic activities and reaction rates of each oligonucleotide in the presence of Mg^{2+}. After 30 min incubation at 37 °C, as shown in figure 18 (B), we found that NonSeq has no activity with *Hin*dIII, showing that the concentration of enzyme in the experiment does not show any significant nonspecific catalytic reaction.

Non-specific strands are known to have different conformations from wild-type dsDNA that inhibits the DNA hydrolysis. In case of *Eco*RV of which is another restriction endonuclease from family of Type II restriction enzyme, the non-specific strand is not distorted enough for magnesium ion to be bound to the substrate and catalyze. A similar assumption can be made for *Hin*dIII.[13]

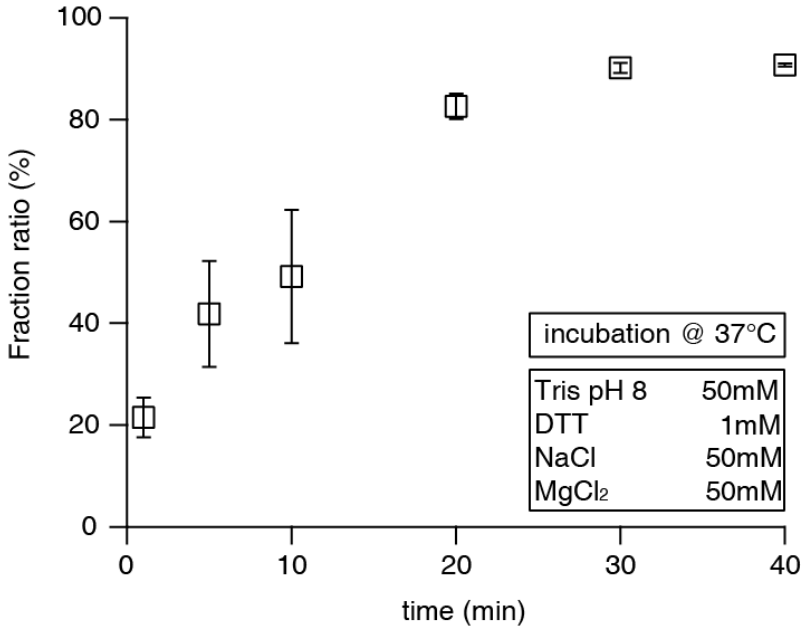

Figure 11. Enzyme activity as a function of time.

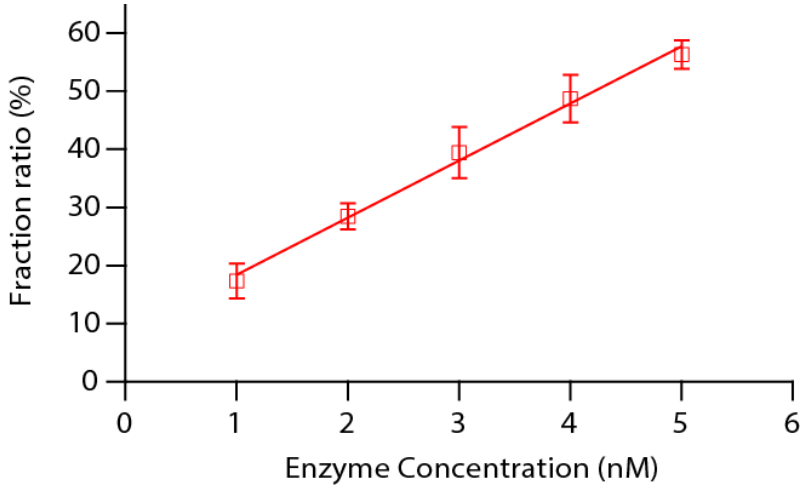

Figure 12. Enzyme activity as a function of enzyme concentration.

3.3.4 Single-molecule test

3-State Kinetics

Figure 13 is a representative data that shows the trace that was obtained for more than 60 seconds and fitted with Hidden Markov Model (HMM). Three transient steps indicate each association and dissociation steps. The lowest state (S1) is the unbound state, the second state (S2) is the first enzyme bound state, and the third state (S3) is when two enzymes are bound to the sequence and results the conformational change. To acquire the trace, Ca^{2+} was used in place of Mg^{2+} because Mg^{2+} functions as a cofactor and cleaves the sequence while Ca^{2+} still helps association of the enzyme but does not cleave the DNA. Enzyme injection causes a repetitive fluctuation of fluorescence. The intensities of the fluctuation seem rather constant. The higher level duration and the lower level duration of many single molecules are represented as a function of occurrences and fitted with exponential decay function: F(t) = Ae^{-kt}.

k is a variable indicating the reaction rate constant. When *k* value increases, the duration is shorter, and vice versa. k_1 is an association rate constant of enzyme, and k_{-1} is a dissociation rate constant and k_{-2} is a rate constant of conformational change refer to the reaction flow figure 6. In figure 14, we collected all the date of a single molecule, and measured the each duration time of S1, S2, and S3 which are related to association, dissociation and conformational change, respectively. The histograms were fitted with single exponential decay function.

Another state S3 is the time duration of conformational change. *Hin*dIII is known as homodimer, and it does not have its nuclease activity unless it forms a dimer. After the proteins are dimerized, they bind to the substrate which later kinks the DNA. *Eco*RV, type II restriction endonuclease, dimerizes and kinks the DNA to ~50° in the presence of metal ion.[14] It is known that *Hin*dIII also kinks the DNA, and distorted when bound with a metal ion.[7] The S3 can be elucidated as another fluorescence enhancement by distortion of DNA.

Enhancement factor of first and the second increment was calculated. The first enhancement factor of S2 state was 1.6, and that of S3 was 1.9. Figure 15 represents the fluorescence intensity increment factor of four different concentrations. The bimodal distribution diagram represents the S1 and S2 states, and the fluorescence enhancement factor is 1.6 at all concentrations. The rate of S3 is too fast having a transient life time that it was not clearly observed in these distributions. When enzyme concentration increases, the association rate (S1) increases as well, which means the higher population of enzyme has a higher possibility of colliding and eventually binding to the DNA. The dissociation rate (S2) was constant that the dissociation rate does not depend on the enzyme concentration.

The enzyme concentration did not influence the intensity ratio between lower and higher level. As it is shown in figure 16, at various enzyme concentrations the ratio between the lower and the higher fluorescence was equal to 1.6.

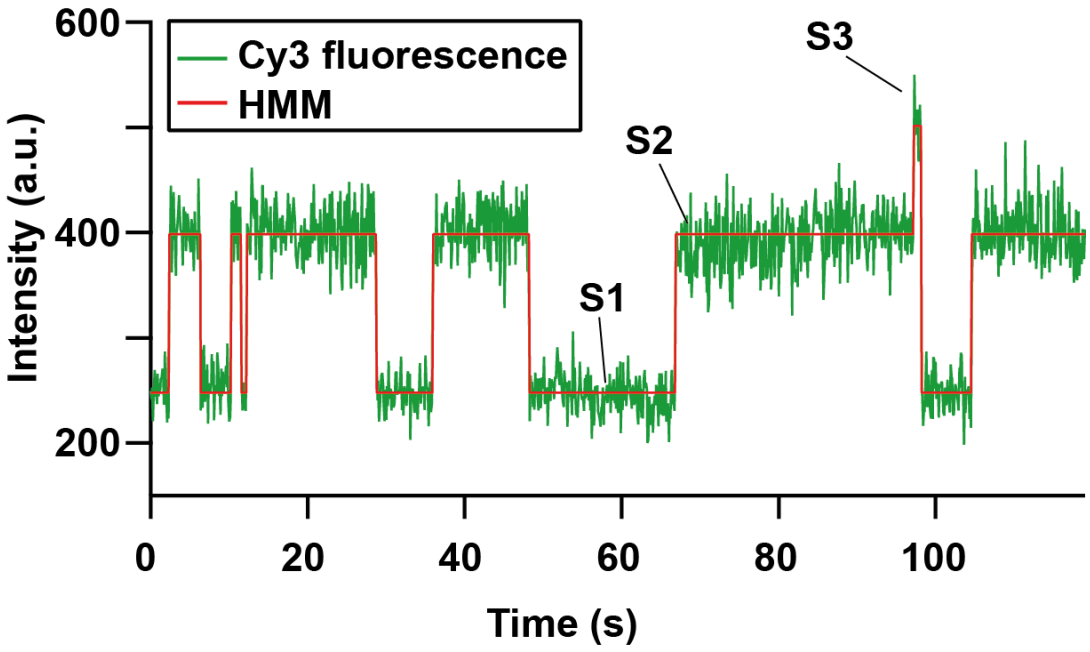

Figure 13. A representative single-molecule fluorescence trajectory. When *Hin*dIII is injected, Cy3 fluorescence on DNA is fluctuating

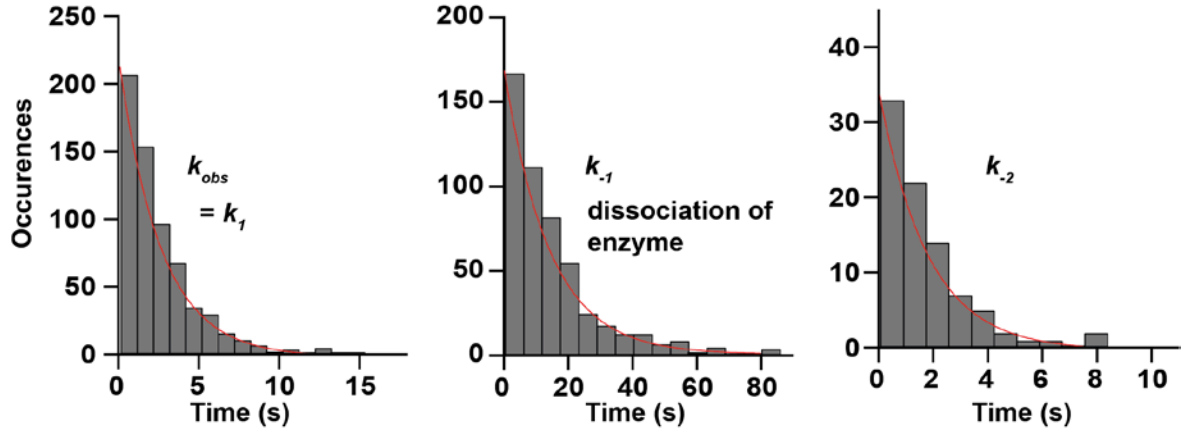

Figure 14. Kinetic analysis for determining rate constants of each reaction step. Example of histograms of the duration times of each reaction step. Histograms were fitted to a single exponential decay curve (red curve).

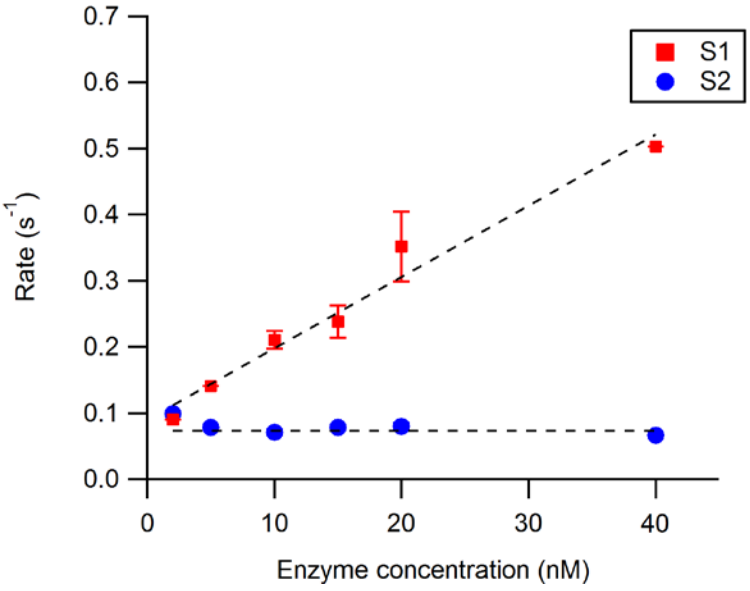

Figure 15. Rate of lower and higher level of fluorescence as enzyme concentration varies. S1 state is a enzyme unbound state, and S2 is a bound state.

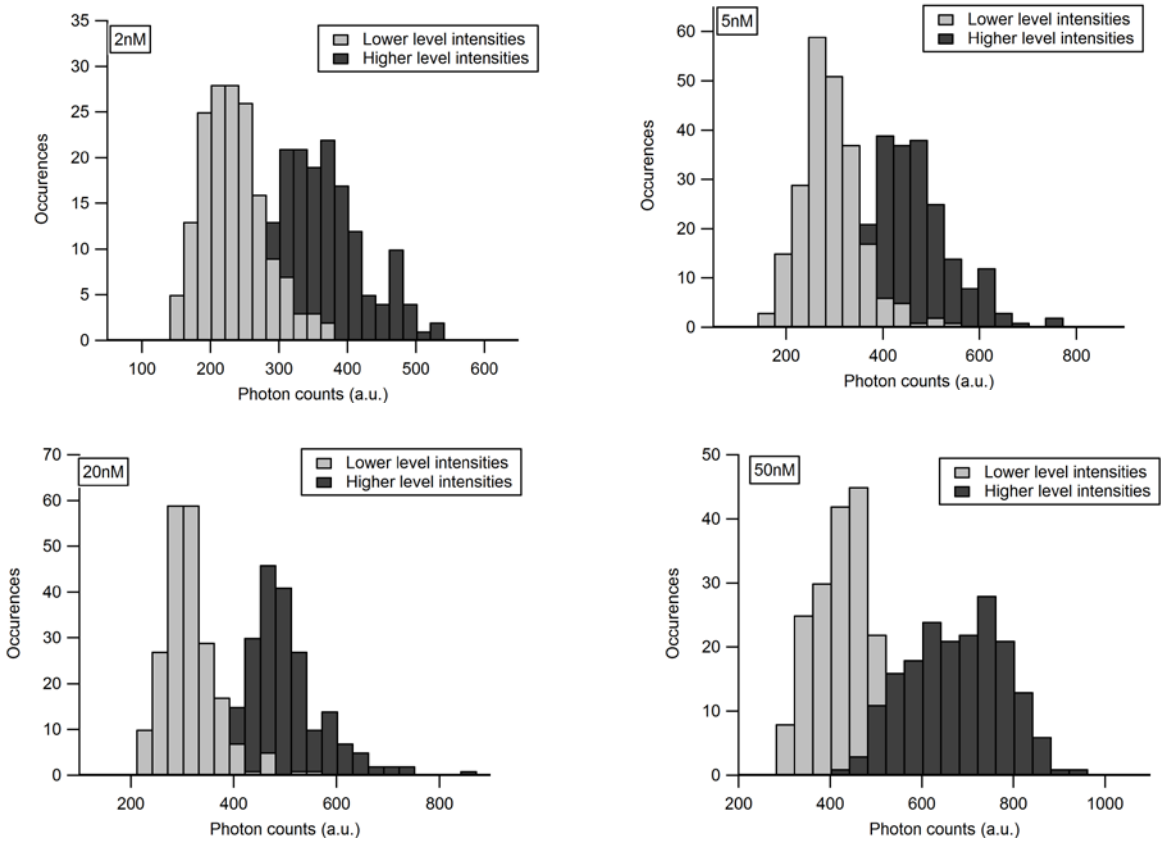

Figure 16. Fluorescence intensity at 2 nM, 5 nM, 20 nM and 50 nM.

Population ratio and equilibrium constant state

Among the rate constants of each reaction step, the measurement of nuclease conformational change rate constant k_2 is so slow that we cannot acquire enough numbers of individual molecules for statics with the conventional single-molecule setup and fluorophores. In order to obtain its value, we introduced the relationship between the equilibrium constant and the concentration of molecules. Now, we consider the chemical equation based on Michaelis-Mentens equation. At equilibrium, the relationship of each chemical reaction rate can be expressed as $k_{on}\cdot[E]\cdot[S] = k_{off}\cdot[E\cdot S]$. We note that if $[E]>>[S]$, the ratio of the concentration ($[E\cdot S]/[S]$) at equilibrium equals the value for $[E]\cdot(k_{on}/k_{off})$. To test the suitability of this kinetic analysis, we compared the ratio of the population (P_{S2}/P_{S1}) and the equilibrium constant (k_{-1}/k_1) of the reaction. As shown in figure 17 (B), we observed similar linear plot. Next, we carried out this analysis to reveal conformational change rate constant k_2.

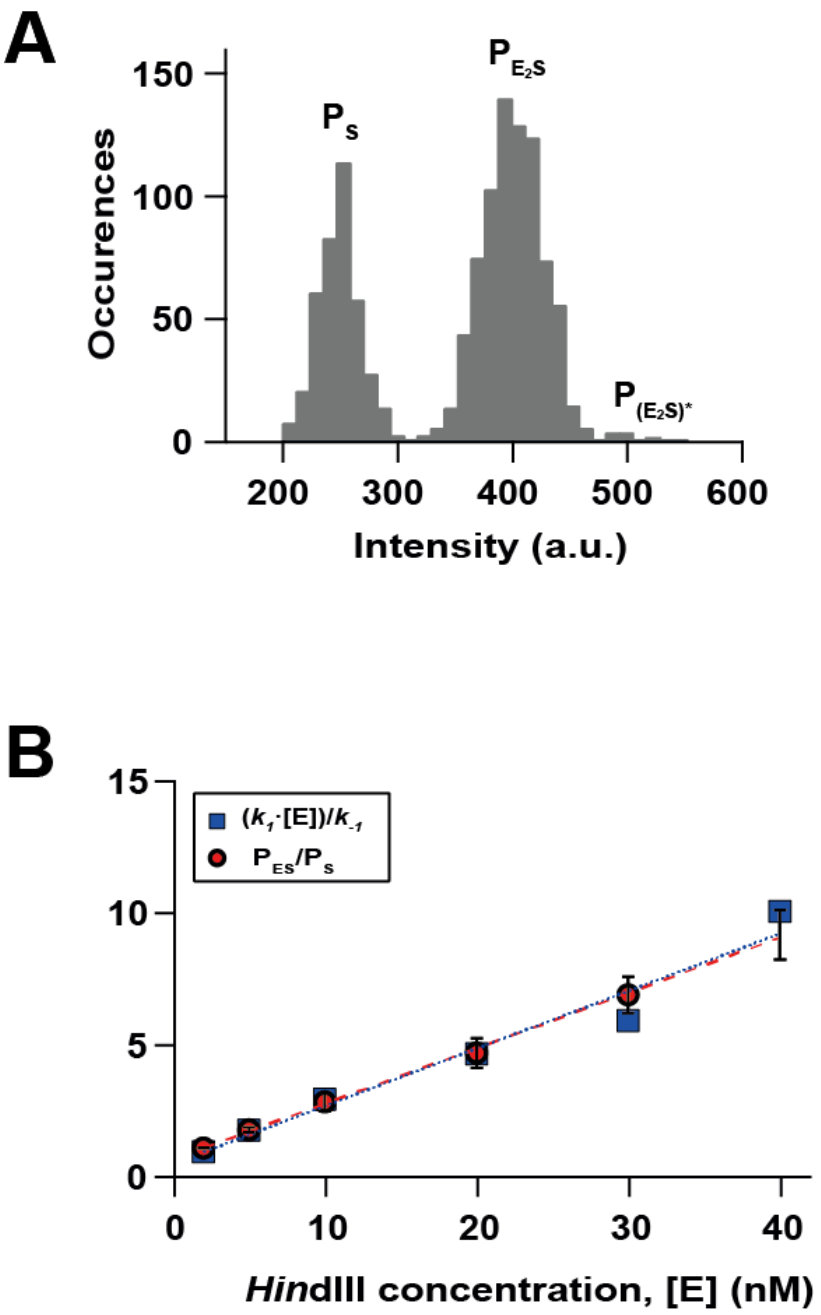

Figure 17. (A) population graph of each state. P_s, P_{ES}, P_{E_2S} are from S1, S2, and S3 state respectively. (B) The population ratio of P_{ES}/P_S.

3.4 Conclusions

First, the kinetics of association and dissociation of *Hin*dIII on DNA was observed by single-molecule technique, TIRF using PIFE effect. The samples were designed to have the most optimal condition to show PIFE effect. By PIFE effect, the fluorescence fluctuates as interacting with the enzymes. The analysis of duration time of high and low level of fluorescence intensity fluctuation was calculated to obtain the association and dissociation rate constants. Thus, the third step of conformational change followed after dimerization was observed.

The optimal conditions for enzyme kinetics were concerned including ion concentration, enzyme concentration, buffer condition, and non-specific binding control tests.

4. Effects of methylation on dsDNA to dissociation protein from dsDNA.

4.1 Introduction

In prokaryotes, native DNA is preserved by methylation. When foreign genes from a bacteriophages are transferred to a prokaryote, methylation of DNA can be a defense against the foreign DNA to keep their native genes.[15] Methylation behaves as a marker that reports not to cleave its native dsDNA. In the meantime, foreign dsDNA are cleaved by restriction endonuclease. Methylation in eukaryotic cells are also closely related to gene regulation and gene expression.[16] Many studies have been done about the effects of methylation but it is still a subject for intense research at a molecular level.

Cytosine of a recognition site (AAGCTT) was hemi- methylated from IDT DNA. Nuclease activity of restriction endonuclease, *Hin*dIII, was tested in ensemble and compared with the wild type (non-methylated), and dsDNA with non-recognition sequence which does not involve specific binding. Through agarose gel result, it was confirmed that when a specific binding sequence is point mutated, protein does not show a nuclease activity, and methylated sequence shows ~10 % less activity efficiency (Figure 18 (B)). When both strands of DNA are methylated at cytosine, there is no nuclease activity (data not shown).

4.2 Results and Discussion

4.2.1. Ensemble test

The enzyme activity was tested with three different substrates: wild type, hemi-methylated, and non-specific sequence DNA. The wild type includes the specific binding site of *Hin*dIII, and the full sequence is in figure 18 (A). The hemi-methylated sequence has a functional group of methyl at the cytosine of the specific binding site. The non-specific sequence DNA has a sequence that does not include the binding site (AAGCTT). The activity of three substrates were tested with an agarose gel, 2 μM DNA were diluted in buffer containing 50 mM of Mg^{2+}, and ~35 nM *Hin*dIII enzyme was added and incubated for 20 min at 37 °C. As a consequence, the fraction ratio which is correlated to the activity of the enzyme reaches over 80% in the case of WT (wild type), and around 70% (hemi-methylated) and almost 0% for the non-specific sequence. It has been confirmed that the non-specific sequence DNA does not show any enzyme activity.

The activity time was also compared between the wild-type and the hemi-methylated type. The reaction condition was the same except, the reaction was stopped by EDTA for every 1 min, 5 min, 10 min, 20 min, 30 min and 40 minuites. The results were clearly distinguishable between two substrates. The wild-type was saturated faster than the methylated one (Figure 18 (C)).

Another control test done to prepare the single-molecule experiment was to confirm that the labeled Cy3 fluorescent dye does not affect the restriction endonuclease activities (Appendix). It was also tested in the same reaction buffer at 37 °C for 20 minutes and clarifies that there is no great difference in the activity between the labeled DNA and non-labeled DNA.

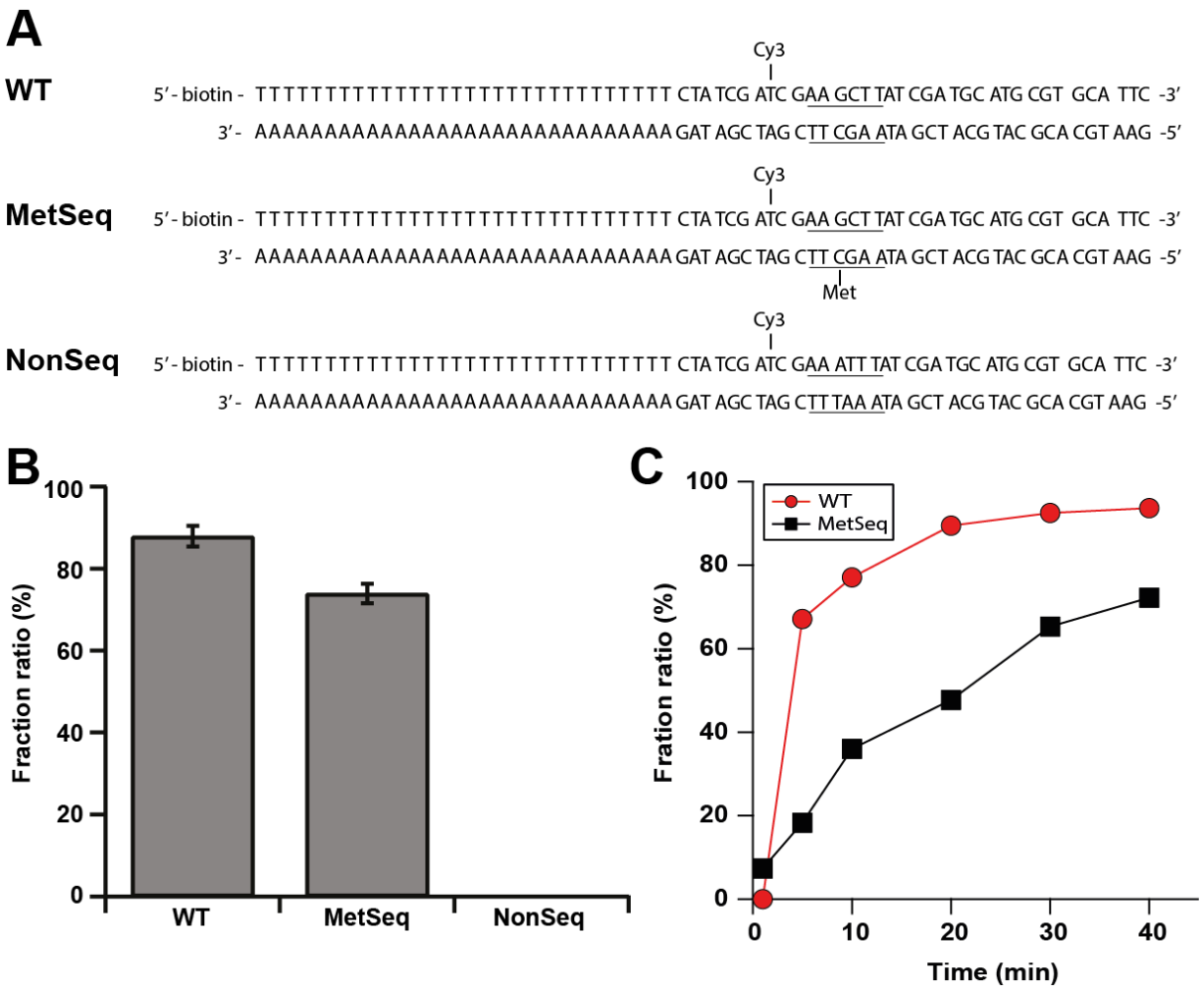

Figure 18. Kinetic difference between WT and MetSeq during the enzymatic catalytic reaction of *Hin*dIII. (A) All oligonucleotide sequences that we used in ensemble and single-molecule measurements. On three oligonucleotides, Cy3 is labeled on the proximal position (3 bps) of *Hin*dIII recognition sequence and biotin is covalently attached on 5' end for immobilizing on the quartz slide. In addition, 5-methylcytosine (5 mC) substituted for a cytosine on the recognition sequence in MetSeq. (B) Ensemble measurement for the enzymatic rate on WT and MetSeq (2 μM) in the presence of 30 nM *Hin*dIII at 37 °C. The catalytic rate of each oligonucleotides can be obtained by fitting with a function, $F(t) = A \cdot (1-\exp(-k \cdot t))$. The k value for WT is 0.194 min^{-1}, and the *k* value for MetSeq is 0.051 min^{-1} (left panel). For 40 min incubation at 37 °C, the cleaved product with MetSeq is ~10 % lower than the product with WT (right panel).

4.2.2. Single-molecule test

We tested three types of methylated DNA substrates: methylated on the both strands on the binding site, hemi-methylated on the Cy3 labeled strand, hemi-methylated on the opposite of the Cy3 labeled strand. The DNA substrate with both strands methylated did not show an activity, but the both hemi-methylated substrates showed a subtle difference in equilibrium constant compared to the methylated type.

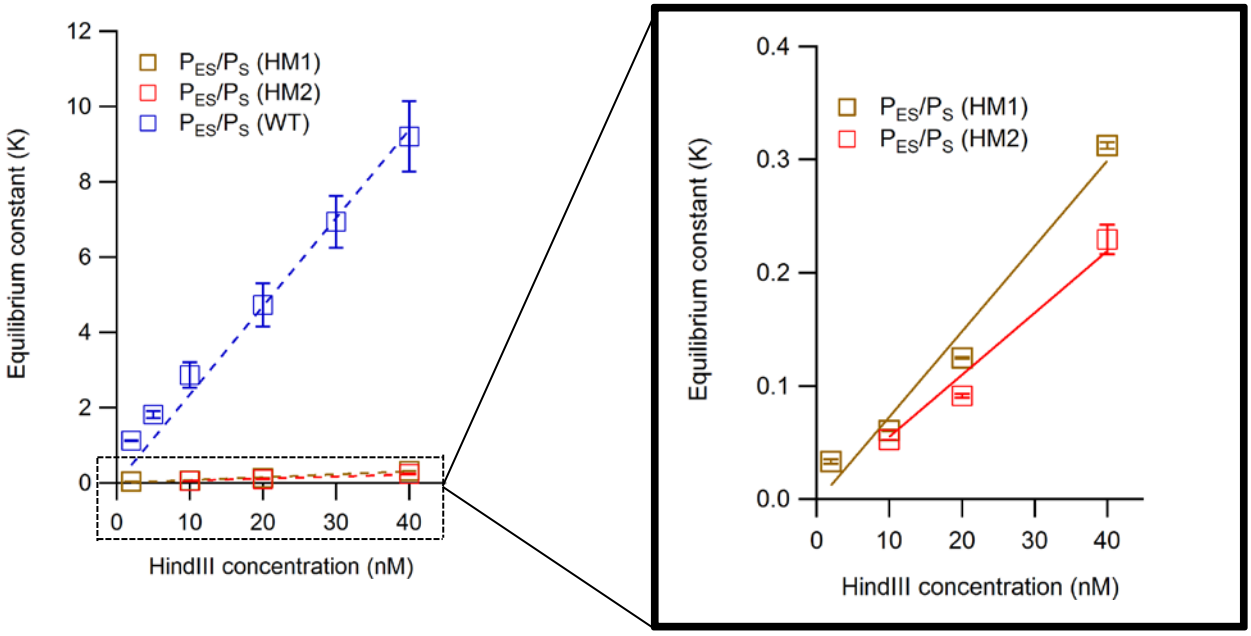

Figure 19. Kinetics comparison between two hemi-methylated substrates. The population ratio from P_{ES} to P_S of hemi-methylated substrate 1 (HM1) and hemi-methylated substrate 2 (HM2) has a small difference, while the wild-type (WT) has a greater equilibrium constant which infers the greater enzyme activity.

The results of protein kinetics against the wild-type DNA and hemi-methylated DNA were utterly different. As shown in figure 19, the wild type DNA and methylated DNA show a main difference in the duration of binding. The binding rates are similar whereas the dissociation rate was much greater in methylated sequence DNA. The duration time of enzyme binding of WT strand with 20 nM at 310 K is about 13.81597, and the duration time of enzyme binding of methylated sequence is about 0.34825. Figure 20 is the representative trace of each wild-type and methylated type substrate. The duration time of bound state has decreased rapidly. The duration time of unbound state was almost the

same as shown in figure 22 (B). The fluorescence enhancement factor was the same as 1.6 as it was observed with WT (Figure 22 (A)). In all experiments, Ca^{2+} was substituted for Mg^{2+} to prevent cleaving.

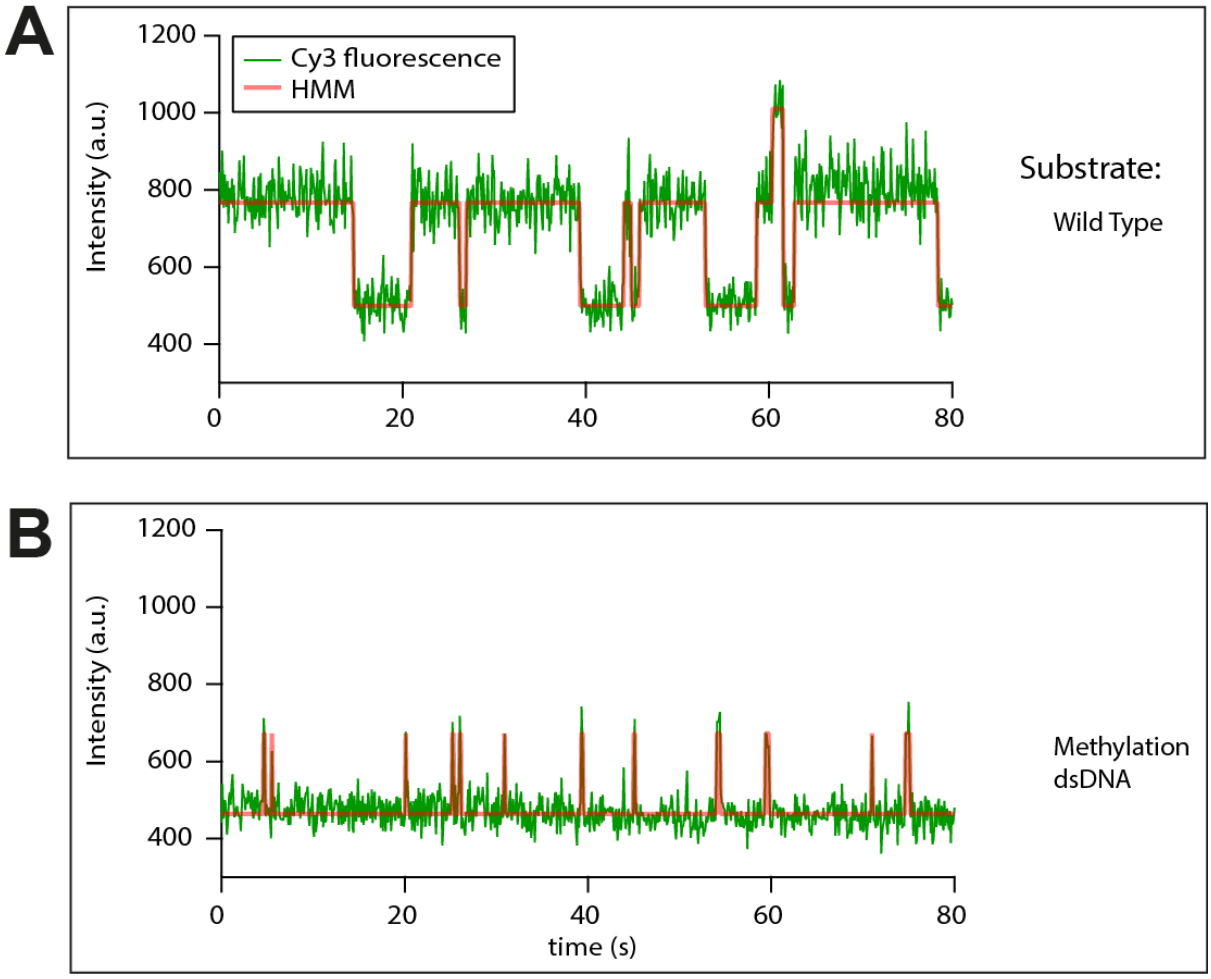

Figure 20. A trajectory of a single molecule. (A) Trace of a Cy3-labeled DNA substrate with *Hin*dIII. The fluorescence is enhanced from 500 a. u. to 800 a.u. The enhanced duration indicates the protein binding in the protein-recognition site. The lower level fluorescence indicates the dissociated duration. (B) Trace of a Cy3-labeled DNA with methylated cytosine in the recognition site. The trace shows a short duration time of the binding of a protein.

4.2.3. Arrhenius plot

Single molecule experiments were repeated in different temperatures; 25, 26, 30, 34, 37 ˚C to understand the thermodynamic properties of the reaction. From the Arrhenius equation (below), the ln *k* vs.1/T plot can be drawn and the activation energy can be calculated from the slope.

$\ln k = \frac{-Ea}{R}\frac{1}{T} + \ln(A)$

k: rate constant, E_a: activation energy, R: Gas constant, T: temperature, A: frequency factor (total number of collisions per second)

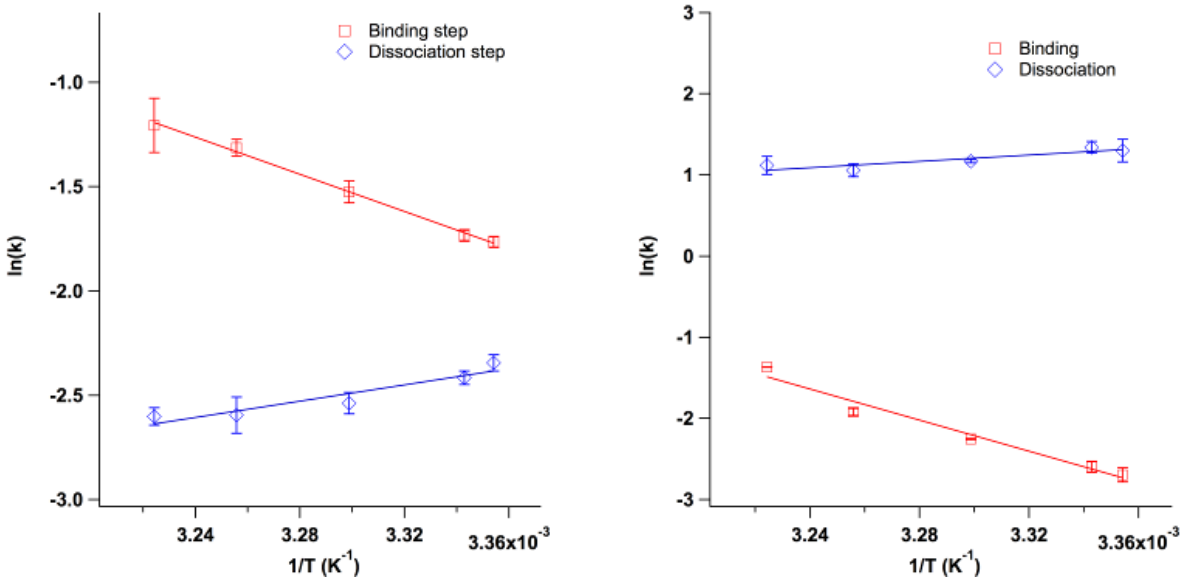

Figure 21. Arrhenius plot. (a) wild type (left) (b) methylated type (right). Single-molecule experiments were tested in 25, 26, 30, 34, 37 °C.

Left is the Arrhenius plot of the wild type (with no methylation) and right is that of methylated type. The activation energy of binding step is 8.874 kcal/K·mol with wild type, and 19 kcal/K·mol in the mythalylated type which can be inferred that thermodynamically it is more difficult to have a enzyme-DNA complex when the nucleic acid is methylated in the middle of the binding site. The gibbs free energy diagram based on the activation energy value can be drawn as figure 22 (C).

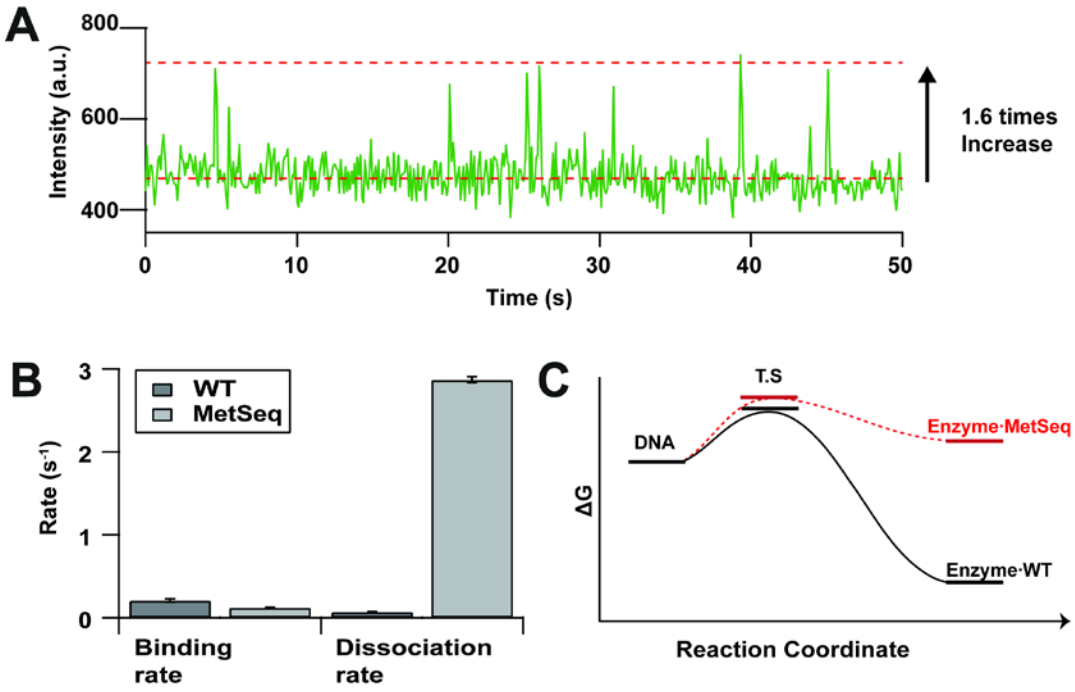

Figure 22. (A) A representative single-molecule fluorescence trajectory. With MetSeq, the 1.6-fold enhancement factor remained, but the duration time of enzyme bound state is dramatically shortening. (B) The comparison of reaction rate between WT and MetSeq. Note that the binding rate on MetSeq is slower than the binding rate on WT, implying the higher activation energy in enzyme binding reaction on MetSeq. (C) Expected free-energy diagram for WT (black curve) and MetSeq (red dashed curve) interacting with enzyme.

4.2.4. Simulation fitted with single-molecule data

The simulation was run with the chemical reaction rate constants obtained from the single-molecule experiments as below.

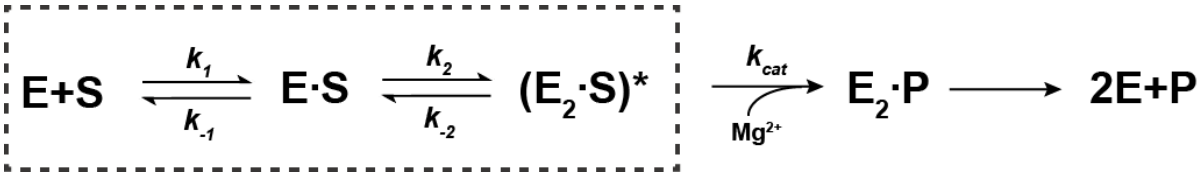

Concentration of E: [E], Initial concentration of E: $[E]_0$, Concentration of S: [S], Initial concentration of S: $[S]_0$ Concentration of ES: [ES], Concentration of ES*: [ES]*, Concentration of product: [P]

$$[E] = [E]_0-[ES]-[ES]^*$$

$$\frac{d}{dt}[S] = -k_1\cdot[S]([E]_0-[ES]-[ES]^*)+k_{-1}\cdot[ES]$$

$$\frac{d}{dt}[ES] = -k_{-1}\cdot[ES]-k_2\cdot[ES]+k_1\cdot[S]([E]_0-[ES]-[ES]^*)+k_{-2}\cdot[ES]^*$$

At equilibrim, $\frac{d}{dt}[ES] = 0$, $\frac{[ES]^*}{[ES]} = \frac{k_2}{k_{-2}} \equiv K_2$

Thus, $\frac{d}{dt}[ES] = -k_{-1}\cdot[ES]-k_2\cdot[ES]+k_1\cdot[S]([E]_0-[ES]-[ES]^*)+k_{-2}\cdot[ES]^* = 0$

$$\rightarrow \frac{d}{dt}[ES] = -k_{-1}\cdot[ES]+k_1\cdot[S]([E]_0-(1+K_2\cdot[ES]) = 0$$

$$[ES] = \frac{k_1\cdot[S][E]_0}{k_{-1}+k_1\cdot[S]+k_1\cdot K_2[S]}$$

$$[ES] = \frac{K_1[S]}{1+K_1[S]}[E0]$$

$k_{cat} \cdot K2 \cdot [ES] \propto d[P]/dt$

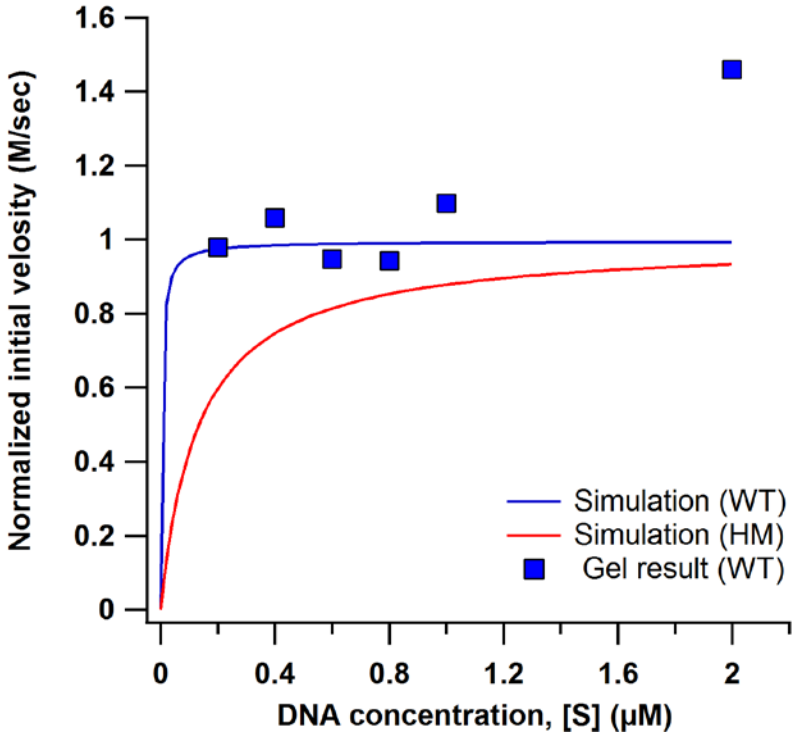

Figure 23 Simulation fitted with single–molecule data. The blue line is a simulation value of a wild-type, and the red line is a simulation value of a hemi-methylated type. The blue points were obtained from the single-molecule tests.

Interestingly, the ensemble agarose gel result was is in accord with the simulation result that was calculated with the single-molecule experiment data. More ensemble experiments are in need to prove the simulation and the assumptions that are counted in.

4.3 Conclusions

DNA methylation does not affect the rate of the binding, but the rate of the dissociation of the enzyme due to its thermodynamically unstability. The ensemble measurement and the single-molecule experiments data converge to the result that helps to understand the kinetics of unmethylated and methylated DNA-enzyme reaction.

5. Reference

1. Axelrod, D., Total internal reflection fluorescence microscopy in cell biology. *Traffic* **2001,** *2* (11), 764-774.
2. Axelrod, D., Cell-substrate contacts illuminated by total internal reflection fluorescence. *The Journal of cell biology* **1981,** *89* (1), 141-145.
3. Hwang, H.; Kim, H.; Myong, S., Protein induced fluorescence enhancement as a single molecule assay with short distance sensitivity. *Proceedings of the National Academy of Sciences* **2011,** *108* (18), 7414-7418.
4. Tomko, E. J.; Fischer, C. J.; Lohman, T. M., Ensemble methods for monitoring enzyme translocation along single stranded nucleic acids. *Methods* **2010,** *51* (3), 269-276.
5. Ha, T., Single-molecule fluorescence methods for the study of nucleic acids. *Current opinion in structural biology* **2001,** *11* (3), 287-292.
6. Pingoud, A.; Fuxreiter, M.; Pingoud, V.; Wende, W., Type II restriction endonucleases: structure and mechanism. *Cellular and molecular life sciences* **2005,** *62* (6), 685-707.
7. Watanabe, N.; Takasaki, Y.; Sato, C.; Ando, S.; Tanaka, I., Structures of restriction endonuclease HindIII in complex with its cognate DNA and divalent cations. *Acta Crystallographica Section D: Biological Crystallography* **2009,** *65* (12), 1326-1333.
8. Nwankwo, D. O.; Moran, L. S.; Slatko, B. E.; Waite-Rees, P. A.; Dorner, L. F.; Benner, J. S.; Wilson, G. G., Cloning, analysis and expression of the *Hin*dIII RM-encoding genes. *Gene* **1994,** *150* (1), 75-80.
9. Pingoud, A.; Jeltsch, A., Structure and function of type II restriction endonucleases. *Nucleic Acids Research* **2001,** *29* (18), 3705-3727.
10. Singal, R.; Ginder, G. D., DNA methylation. *Blood* **1999,** *93* (12), 4059-4070.
11. Tang, D.; Ando, S.; Takasaki, Y.; Tadano, J., Mutational analyses of restriction endonuclease—HindIII mutant E86K with higher activity and altered specificity. *Protein engineering* **2000,** *13* (4), 283-289.
12. Selvin, P. R.; Ha, T., *Single-molecule techniques: a laboratory manual*. Cold Spring Harbor Laboratory Press Cold Spring Harbor, NY: 2008.
13. Berg, J. M.; Tymoczko, J. L.; Stryer, L., *Biochemistry, International Edition*. WH Freeman & Co. New York: 2006.
14. Winkler, F. K.; Banner, D. W.; Oefner, C.; Tsernoglou, D.; Brown, R.; Heathman, S.; Bryan, R.; Martin, P.; Petratos, K.; Wilson, K., The crystal structure of EcoRV endonuclease and of its complexes with cognate and non-cognate DNA fragments. *The EMBO Journal* **1993,** *12* (5), 1781.
15. Jeltsch, A., Beyond Watson and Crick: DNA methylation and molecular enzymology of DNA methyltransferases. *Chembiochem* **2002,** *3* (4), 274-293.
16. Reik, W., Stability and flexibility of epigenetic gene regulation in mammalian development. *Nature* **2007,** *447* (7143), 425-432.
17. Shi, X.; Lim, J.; Ha, T., Acidification of the oxygen scavenging system in single-molecule fluorescence studies: in situ sensing with a ratiometric dual-emission probe. *Analytical chemistry* **2010,** *82* (14), 6132-6138.

Appendix

6. Optimal Condition for enzyme activity

6.1 Ion concentration

To find the most optimal condition for the enzyme activity, concentrations of $MgCl_2$ and NaCl were controlled. Enzyme activity highly depends on the Mg^{2+} ion concentration (Figure 24). Enzyme activity of catalytic was most activated when Mg^{2+} was 50 nM. NaCl was also tested and verified that sodium ion concentration does not affect the enzyme activity. To test the effect of monocation, KCl was substituted for NaCl. KCl concentration also did not show dependence on enzyme activity (Figure 25). The first column of figure 25 represents the best combination of the ion concentration for the enzyme activity. As it demonstrates, the enzyme activity which is correlated with the fraction ratio is the highest with 50 nM of Mg^{2+}, whereas sodium, or potassium ion has no effects on the activity.

6.2 Reaction in imaging buffer

In ensemble test, the enzyme activity was most activated in the buffer containing 50 mM Tris pH 8.0, 50 mM MgCl2, 50 mM NaCl, and water. In single-molecule test, the buffer condition is different because Trolox, glucose, pyranose oxidase, and catalase were used to visualize the fluorescent molecules. Molecular O_2 causes photobleaching which disturbs the observation of the kinetics of a fluorescent dye. Glucose and pyranose oxidase are the oxygen scavenging system that eliminates the oxygen.[17] Also with the oxygen scavenging system, Trolox is used to reduce photobleaching.[17] To examine the effect of the imaging buffer, enzyme was incubated in each buffer for 10 minutes at 37 °C. In figure 26, it confirms that IB does not affect the enzyme activity. The fraction ratio demonstrates the amount of dsDNA that was cleaved by *Hin*dIII. It was measured by ImageJ.

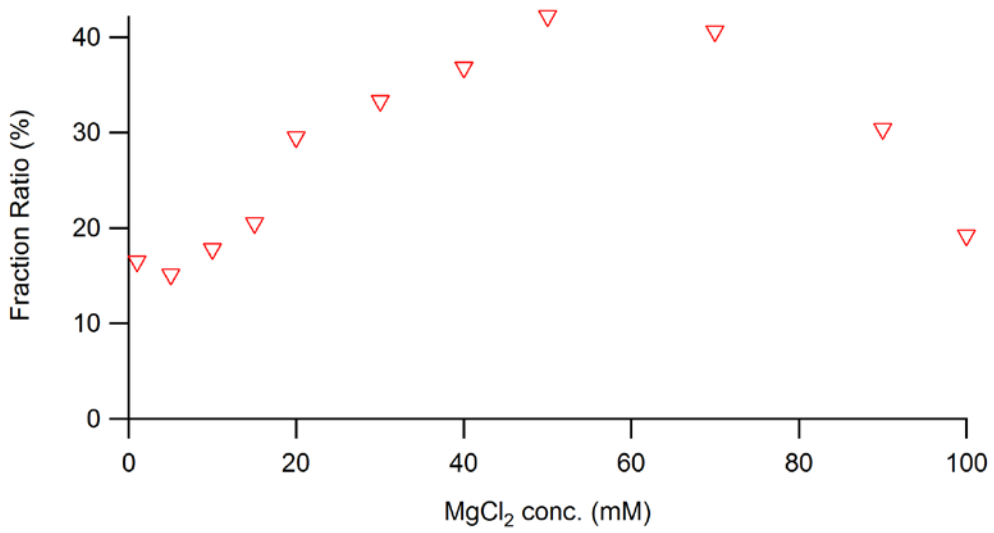

Figure 24. Mg^{2+} ion dependence on *Hind*III enzyme activity. The reaction was run in buffer with 50 mM of NaCl for 30 minutes at 37 °C.

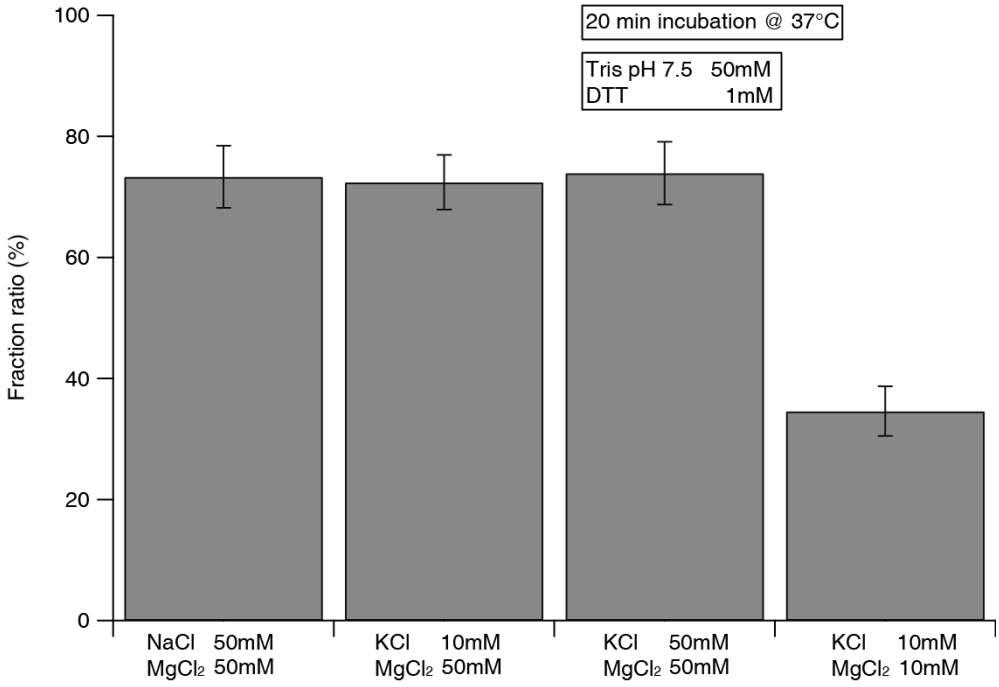

Figure 25. Ion dependence on enzyme activity. Various concentrations of NaCl, and KCl were tested for enzyme activity.

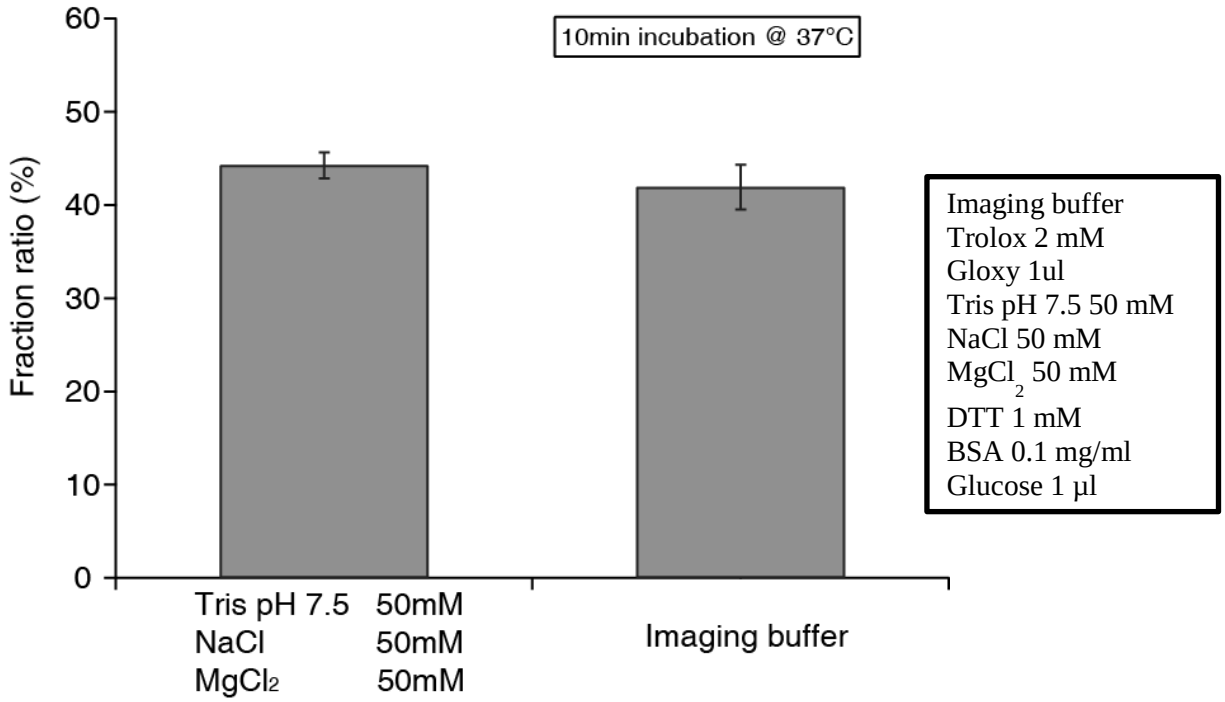

Figure 26. Enzyme activity test in imaging buffer. Imaging buffer including triplet quenchers is mandatory in single-molecule experiments.

6.3 Enzyme activity on wild type vs. fluorophore labeled dsDNA

Cy3 fluorophore is labeled at 3bp far from the recognition site of the enzyme (AAGCTT) which can block the enzyme binding or disturb the interaction of the dsDNA – protein. Prior to the TIRF single-molecule test, it was necessary to test the effect of Cy3 fluorophore labeling. In figure 27, a control sample was B which both ssDNA do not have any modifications. A is the sample with Cy3 labeled on one strand of the labeled substrate. Both samples (~2 μM) were incubated in a buffer with enzyme (~35 nM) at 37 ˚C for 20 minutes. The labeled substrate shows less than 10 % lower enzyme activity. The third lane is enzyme activity of the wild type substrate without Mg^{2+} ion in reaction buffer. The enzyme does not appear to have any endonuclease activity without Mg^{2+} ion.

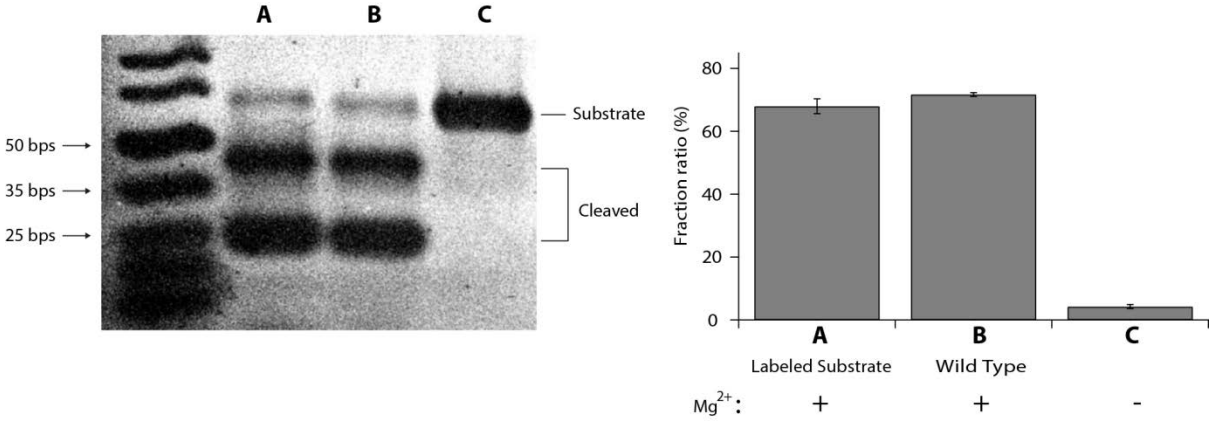

Figure 27. Effects of fluorophore labeled strand on *Hind*III enzyme activity. A lane represents the substrate which is labeled with Cy3 flurophore on 3bp far from the recognition site, B lane represents the wild type substrate with no modifications and C lane represents the wild type substrate in buffer without Mg^{2+} ion. A and B lane show three bands of cleaved fragments. Each fragment demonstrates 66 bp (full length), 25 bp and 41bp. C lane shows no activity of enzyme.

6.4 Time trajectory of a single molecule.

A time trajectory of a single Cy3-labeled substrate shows the fluctuations as the enzyme was injected to a reaction chamber. After about 70 seconds of constant fluctuations, the Cy3 fluorescent dye was quenched and shows no more signals. This trace provides several information about the DNA-enzyme interaction. First, enzyme injection indeed increases the intensity of fluorescence in a regular base. Second, the fluorescence intensity enhancement factor is constant. Third, the substrate and enzyme concentration was appropriate to avoid the overlapping of fluorophores.

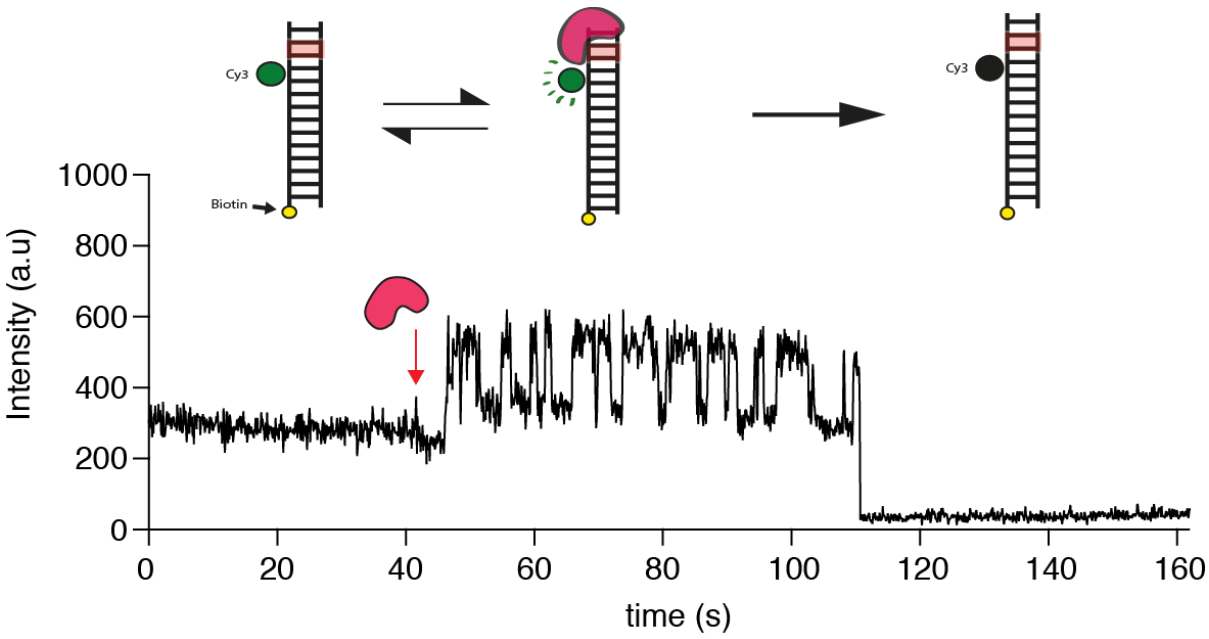

Figure 28. Time trajectory of a single molecule. *Hin*dIII was injected after 40 seconds, and the after the fluorescence fluctuations, the dye quenched at 110 seconds.

국문초록

DNA 매틸화는 진핵생물 세포와 원시핵 생물 세포 내에서 모두에서 중요한 역할을 하고 있습니다. 진핵 생물에서는, gene regulation 을 조절하기도 하고, 원시핵 생물 특히 박테리아에서는, 외부로부터 침입하는 유전자로부터 자신을 지키는 역할을 하기도 합니다. 지금껏, DNA 매틸화에 대해 많은 연구가 되어 오고 있지만, 대부분이 ensemble 수준에서 연구된 것입니다. 이번 연구에서 우리는 DNA 매틸화가 DNA 와 단백질관의 상호관계에 주는 영향에 대해 단분자 수준에서 연구하고자 합니다. 단백질이 DNA 에 붙고 떨어지는 속도를 구하여서, DNA 가 매틸화 되어있을 때 붙고 떨어지는 속도를 비교하였습니다. 또한, 단분자 수준에서 구한 동역학적 값들이 ensemble 수준에서 값으로 수렴하는 것을 볼 수 있었습니다. 더 나아가, DNA 가 매틸화 되어있을 때는 동역학 매커니즘의 특정 부분이 영향을 받는 것으로 밝혀졌습니다.

주요어: 단분자 테크닉, 전반사 형광 현미경, 제한 효소, *Hind*III, DNA−단백질 상호작용, DNA 매틸화

학번: 2011−23221